# *GENOME-WIDE PHYLOGENETIC RECONSTRUCTION FOR PROCELLARIIFORM SEABIRDS IS ROBUST TO MOLECULAR RATE VARIATION*

ANDREA ESTANDIA

# GENOME-WIDE PHYLOGENETIC RECONSTRUCTION FOR PROCELLARIIFORM SEABIRDS IS ROBUST TO MOLECULAR RATE VARIATION

**Andrea Estandía**

**A thesis submitted for the degree of Master of Science by Research**

**Department of Biosciences, Durham University**

**2019**

## ABSTRACT

Substitution rates are known to vary across a wide range of organisms, including birds. Physiological and life-history traits that correlate with body mass may be responsible for differences in substitution rate, which can lead to inaccurate reconstructions of evolutionary relationships and obscure the true phylogeny of affected clades. Given the striking 900-fold difference in body mass between the smallest and largest members of the order Procellariiformes, which encompasses petrels, storm petrels and albatrosses, we used genome-scale nuclear DNA sequence data from 4365 ultraconserved element loci (UCEs) in 51 procellariiform species to examine whether phylogenetic reconstruction using massive genome-wide datasets is robust to the presence of extensive rate heterogeneity. In effect, branch length variation in our phylogenetic trees evidences rate variation. Despite this, all phylogenetic analyses (Maximum-likelihood, Bayesian inference and species tree) recovered the same branching topology, including those constrained to have uniform, clock-like substitution rates and those implementing a relaxed clock model that allows rates to vary among lineages. Using Phylogenetic Generalised Least Squares tests, we found that body mass and age at first breeding together explain 64% of the variance in substitution rate. The inferred topology provides a backbone phylogeny for procellariiform seabirds and resolves several controversies about the evolutionary history of the order. We find that the albatrosses are basal, and that the two lineages of storm petrels are not sister to each other. We also find the diving petrels, which have previously been hypothesised as a distinct family, are nestled within the Procellariidae.

# CONTENTS

## LIST OF ABBREVIATIONS

AFB – Age at first breeding

AIC – Akaike information criterion

AICc – Akaike information criterion corrected for small sample sizes

BF – Bayes factor

BI – Bayesian inference

bp – base pair

ESS – Effective sample size

DNA – Deoxyribonucleic acid

GHOST – General Heterogeneous evolution On a Single

Topology GTR – Generalized-time reversible

HKY – Hasegawa-Kishino-Yano

ILS – Incomplete lineage sorting

LBA – Long branch attraction

NJ – Neighbor-Joining

MCMC – Markov chain Monte Carlo

ML – Maximum likelihood

MLE – Marginal likelihood estimation

MP – Maximum parsimony

PGLS – Phylogenetic generalized least squares

PP – Posterior probability

SD – Standard deviation

SWSC-EN – Sliding-Window Site Characteristics based in Entropy

UCE – Ultraconserved element

## DECLARATION AND STATEMENT OF COPYRIGHT

I declare that no part of this thesis has previously been submitted for a higher degree and that the work presented in this thesis is the result of my own work.

## ACKNOWLEDGEMENTS

There are so many people who I would like to thank for their support that I think I'm not going to be able to fit everyone in one page.

I would like to thank Andreanna Welch who has been my supervisor and friend during this journey. She has transmitted me her passion in every conversation. She has always been keen to help me, to chat at any time and to listen to me patiently. She has been extremely supportive during my time at Durham and even more when I moved to Vienna and focusing on writing up was not easy. I only hope to work with her again someday.

I would also like to thank my collaborators Helen James and Terry Chesser, from the Smithsonian Institution and the USGS. They always gave invaluable feedback. Helen invited and funded my trip for attending the Pacific Seabird Group meeting in Kauai, Hawaii, where I had the opportunity to present our research and spend an awesome holiday birdwatching with Terry and snorkelling with Gabriela and friends (turtles).

I could not have done this without the support of my lab mates and friends. Rus Hoelzel was the head of the Molecular Ecology group at the Biosciences Department and I want to thank him for chatting with me when I needed. I want to especially thank Menno, Erandi and Monica for being always in the good and bad moments. Menno helped me a lot with the coding. Erandi and Monica always satisfied my desire for Mexican food. Joan got me started with the UCE analysis. Also thanks to Max, Thomas, Biagio, Sofia, Nico, Consuelo, Charlotte, Ryan, Aline, Ciprian, Gemma, Andrea, Vania, Jeroen, Angus, Federica, Alejandro and many others. I am incredibly lucky to have so many wonderful people around. I also would like to thank my family and my partner's family for suffering with me during the bad times and trying very hard to understand what I do!

Finally, I would like to thank Nilo. I want to thank him for all the incredibly long and exciting conversations about evolution and particularly about the matters of this thesis. Also, I thank him for his help with the figures. This last year has been great by his side and I hope we can keep enjoying each other's company and making science together for many years more. I dedicate this thesis to him.

# CHAPTER I. INTRODUCTION

## 1.1 The order Procellariiformes

### *1.1.1 An introduction to the order Procellariiformes*

Albatrosses and petrels are the 'seabirds of the open ocean' (Brooke 2004). They often appear mysterious, as are the oceans they roam, and often play an important symbolic role in nautical myths and beliefs. *The Rime of the Ancient Mariner,* by Samuel Taylor Coleridge, tells a story about a sailor who was unlucky to kill an albatross and was forced by his fellow sailors to wear the bird's body around his neck. Mariners also believed that petrels did not approach land and when they laid an egg they carried it under their wings (Simmons 1927).

The order Procellariiformes comprises the albatrosses, storm-petrels, diving petrels, gadfly petrels, shearwaters, fulmarines and prions (Fig. 1). The name is derived from the Latin *procella* meaning storm, tempest or gale. This group is the most diverse lineage of oceanic birds and includes a 900-fold difference in body mass between the smallest and largest of its 120+ species (Fig. 2).

**Figure 1.** Illustrations of a representative species of each of the main lineages within the Procellariiformes. Albatrosses (top) and diving-petrels, gadfly petrels, southern and northern storm-petrels (from bottom-left to bottom-right). Illustrations reproduced from Brooke 2004.

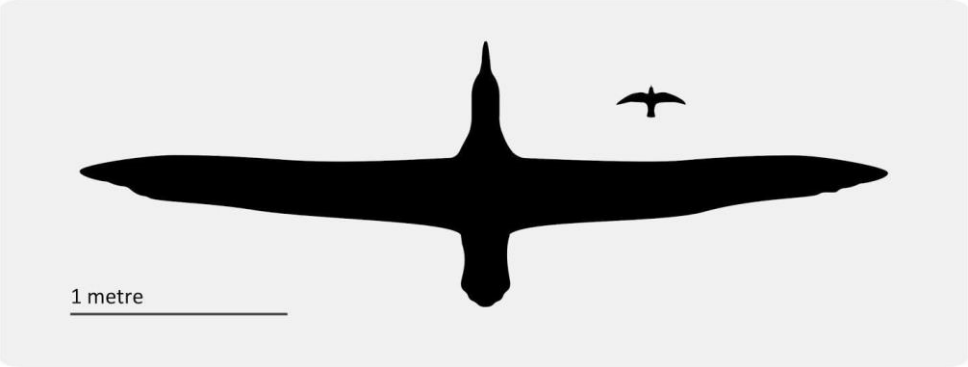


**Figure 2.** Least storm-petrel (*Oceanodroma microsoma*) wingspan (36 cm) vs Wandering albatross (*Diomedea exulans*) wingspan (3.5 m), to scale. Body weight in procellariiformes ranges from 14 g to 16.1 kg.

The morphological traits of this group are generally highly conserved. Plumage patterns usually contain a combination of black, white, grey, and sometimes brown. Procellariiformes are mainly monomorphic with a few exceptions within the albatrosses, and giant petrels and albatrosses are the only groups that change plumage colour with age. The tubular nostril is the most characteristic trait that diagnoses this group of birds. It provides another popular name to designate the order: Tubinares or tubenoses. The tubular nostril is used for olfaction and together with well-developed olfactory bulbs of the brain Procellariiformes are capable of identifying their nests, mates, and locating food at sea (Bonadonna et al.2003).

Life for birds in the oceanic realm appears to place certain constraints on morphology, physiology, behaviour, and life history, just as it does for marine mammals. For example, all oceanic seabirds including Procellariiformes are marine predators and many of them have the ability to fly great distances over the oceans. Some procellariiform species are well-known by their long-distance trans-equatorial migration (Brooke 2004). This is the case of the sooty shearwater, which migrates from New Zealand and Chile to the North Pacific, spanning an annual round trip of 64000 km (Shaffer et al. 2006). Procellariiformes show high levels of natal and site philopatry, and after migrating such long distances they are capable of finding the same nest site every year. Their navigation accuracy has been studied by Welsh ornithologist Ronald Lockley with a series of experiments where he found that the shearwaters flew a straight line “under a clear sky”. However, if clouds were present the shearwaters flew around disoriented and sometimes did not find the way back to the nesting island (Lockley 1967). Despite the constrains that

ecology pose to these birds, they show a range of morphological characteristics (e.g. extreme variation in body size) and foraging strategies (Wang and Clarke 2014), from solitary foraging over the open ocean to foraging in mixed flocks or in association with other marine predators, such as tuna (Schreiber and Burger 2002). Their flight strategies are also diverse, ranging from dynamic soaring by albatrosses to plunge diving by shearwaters. Procellariiformes live in colonies that can vary in density from widely spaced in giant petrels to very dense colonies in storm-petrels (Brooke 2004). Colonies are mostly located on remote and inaccessible oceanic islands, although some species can nest on the mainland and close to human settlements, such as the northern fulmar colony located in the town of St Andrews in Scotland. They are monogamous and form long-term pair bonds, in some cases lasting their whole lives. Courtship comprises several performances such as preening, beak clacking, pointing, calling and 'sky-calling' (Pickering and Berrow 2001). They invest extensive parental care in a small number of chicks even after fledging (Brooke 2004) and they live a long time (from seven to 40 years in average (Douglas and Fernandez, 1997) although 'Wisdom', a Laysan albatross hatched at the Midway Atoll National Wildlife Refuge is currently 68 years old and still successfully rearing offspring).

### *1.1.2 Conservation status*

As Procellariiformes are one of the main marine predators, they have been used as bioindicators of marine productivity and food availability (Inniss et al. 2016). However, they comprise one of the most endangered groups of birds – the percentage of threatened procellariiform species is much higher than Aves overall (Rodriguez et al. 2019). Currently about the 44% of the recognised procellariiform species are classified as Critical, Endangered or Vulnerable by the International Union of the Conservation of Nature (IUCN 2011; Croxall et al. 2012; Borrelle et al. 2016; Rodriguez et al. 2019). Within the order, the Family Procellariidae is the most affected with the genera *Pterodroma* and *Pseudobulweria* standing out as the groups that include the highest percentages of endangered species (Inniss et al. 2016).

Procellariiformes face threats at terrestrial breeding colonies from alien invasive predators, habitat degradation, and human disturbance, and at sea from commercial fisheries, pollution, and global climate change (Croxall et al. 2012; Sydeman et al. 2012). Introduced terrestrial predators are one of the main threats because the typical procellariiform period of parental care is long and birds nest on the ground or in burrows,

where predators have the opportunity to attack and kill the young. Additionally, most species of Procellariiformes only produce a single chick per breeding period, and breeding periods may be annual or biannual. Although some predators focus only on chicks, others like rats (*Rattus* sp.) can predate at any life stage, contributing to the low survival ratio (Borrelle et al. 2015).

Oceanic plastic pollution may be the most widely known threat to seabirds and particularly to Procellariiformes. It is predicted that 99% of all marine species will ingest debris by 2050, but Procellariiformes are currently showing the highest frequency of debris ingestion (Wilcox et al. 2015). A single case of debris ingestion causes a 20.4% chance of mortality and ingestion of >90 items causes a 100% chance (Roman et al. 2019). Luckily, news agency and social media campaigns have been raising public awareness of these issues, though it continues to be a problem (Loughrey 2018).

### 1.2 Phylogenomic inference methods

Phylogenetics is the study of the evolutionary relationships between biological units (Thain & Hickman, 1995) with the aim of reconstructing a 'tree of life'—an analogy that represents bifurcating lineages descending from a single common ancestor in the manner of branches coming off the trunk of a tree (O'Malley et al. 2010).

Phylogenies that were previously built by only scoring morphological characters were improved during the 1980's, when Sanger sequencing and PCR were developed and obtaining DNA became possible. Convergent evolution is a frequent problem of using exclusively morphological data which may lead to the wrong phylogenetic tree. More recently, molecular phylogenetics has made use of new, increasingly fast and cheap genome-sequencing techniques, known as next generation sequencing (NGS). Thanks to these new technologies, the amount of available genetic data has dramatically increased during the last decade.

The statistical inference methods used to reconstruct phylogenies have changed rapidly, too. Maximum parsimony (MP) and distance-based methods (e.g.,neighbour-joining and minimum evolution) were once popular, but have been criticised for not properly accommodating well missing data. They have also shown unreliable results due to systematic errors such as long branch attraction (LBA) by which taxa with long branches falsely appear to be closely related; LBA is particularly troubling for MP (Criscuolo et al. 2006; Wiens et al. 2008). They have been substituted by methods such as

maximum-likelihood (ML) and Bayesian inference (BI), which, notwithstanding their higher computational demands, have been shown to be more reliable (Holder and Lewis 2003).

ML uses probabilities of observing the data (D) given the model (M):P(D|M). The resulting likelihood is the probability of the observed data (i.e. sequences) given a specific model of evolution and tree.

BI methods are similar to ML approaches but incorporate prior probabilities (i.e. a set of prior assumptions about the data matrix to infer the probability that a hypothesis may be true) (Woolrich et al. 2009). Prior probability distributions need to be assigned and the posterior probability (PP) is calculated according to Bayes'theorem:

$$P(H|E) = \frac{P(E|H)P(H)}{P(E)}$$

- P(H | E) – PP of H given E.
- H – hypothesis.
- E – Evidence
- P(H) – prior probability of H that was inferred before new evidence: E became available.
- P(E | H) – probability of seeing E if the hypothesis H istrue.
- P(E) – *a priori* probability of seeing E under all possible hypotheses.

The Markov chain Monte Carlo (MCMC) algorithm (Metropolis et al. 1953), particularly the Metropolis-Hastings algorithm, is the most common method for randomly sampling from probability distributions in phylogenetics (Nascimiento et al. 2017). This algorithm forms a chain of locations in parameter space and the chain moves through it exploring different trees and models of evolution. If by changing the parameters in a new location the PP is higher, the new location is accepted as the new starting point. However, if the new location is rejected, the same location is used again as the starting position. This process is repeated millions of times. The search tends to stay in areas of high PP, which are thoroughly searched. At the end of the analysis the result is an estimate of the PP of the given tree being accurate (Holder & Lewis 2003). BI gives the PP of each clade as a measure of statistical support (Heulsenbeck & Ronquist 2001).

### 1.3 Systematic biases in phylogenetics

Even though the inference methods used in phylogenetics are increasingly more sophisticated, errors and biases are still very common. Genomic data can drastically reduce stochastic errors that arise as a result of the limited amount of information available from genetic or morphological studies (Philippe et al. 2011). However, systematic errors are dependent on the inference methods and quality of the input data and therefore they are present even when applying genome-wide data (Delsuc et al. 2005).

Incomplete lineage sorting (ILS) is one of the most common biases in phylogenetics. It occurs when a polymorphic ancestral species diverges into two daughter species which retain some ancestral polymorphism. When one of these daughter species diverges again, the gene tree at that locus may not coincide with the species tree and species that are not closely related may falsely appear to be (Fig. 4). Especially in periods of rapid divergence, the phylogenetic signal tends to be very low and therefore relationships may be difficult to decipher. Also, when characters have experienced multiple changes, phylogenetic signal may be masked due to homoplasy (a character shared by a set of species but not present in their common ancestor).

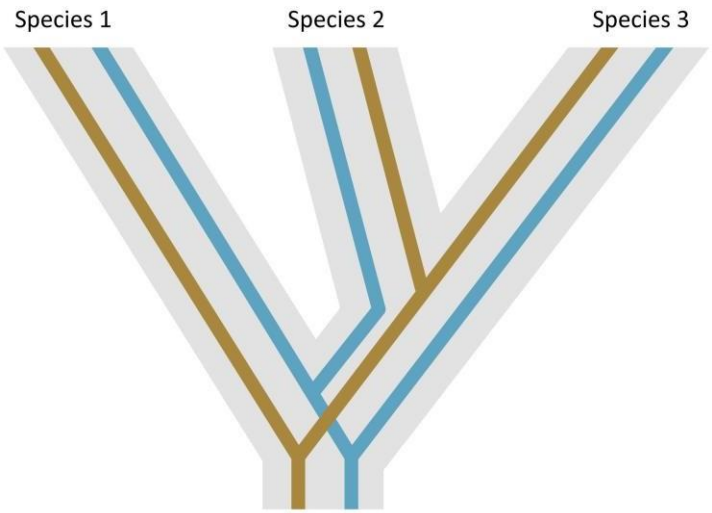


**Figure 4.** Species 1 and Species 2 may seem to be closely related than Species 2 and Species 3 due to ILS.

Although some studies still propose a universal clock-like substitution rate across the Tree of Life (e.g. Weir and Schluter 2008; Brown and Yang 2011; Hedges et al. 2015), substitution rates have been shown to be highly variable across a number of lineages (e.g. Pereira and Baker 2006; Patané et al. 2009; Eo and DeWoody 2010; Beaulieu et al. 2015). Most biologists accept a constant nucleotide substitution rate across very closely related taxa (i.e. congeners; Li 1993, although see Dornburg et al. 2014; Ho 2014), but would argue that a similar rate of nucleotide substitution is unlikely to coincide in evolutionarily distant groups (Tamura et al. 2012). Rate heterogeneity leads to differences in reconstructed branch lengths that can obscure true evolutionary relationships (Felsenstein 1978; Hendy and Penny 1989; Anderson and Swofford 2004). Although rate of substitution is a fundamental issue in phylogenetics, there is a lack of consensus regarding the mechanisms that play a role in shaping rate heterogeneity across taxa at different taxonomic scales (Field et al. 2019).

Hypothesised causes of rate heterogeneity include disparities in metabolic rate, body size, and life history traits such as generation time (Martin and Palumbi 1993; Mooers and Harvey 1994; Nabholz et al. 2009). In most cases, small-bodied animals have been found to have higher rates of substitution than large-bodied animals (e.g. Welch et al. 2008, but see Lanfear et al. 2010 and Thomas et al. 2010). Body size has been linked to mitochondrial substitution rate (reptiles: Bromham 2002; mammals: Steiper and Seiffert 2012; birds: Nabholz et al. 2013) and nuclear substitution rate (reptiles: Bromham 2002; birds: Jarvis et al. 2014; Weber et al. 2014; Berv and Field 2018). Generation time (invertebrates: Thomas et al. 2006; flowering plants: Smith and Beaulieu 2009), longevity (fish: Hua et al. 2015), and metabolic rate (birds: Berv and Field 2018) have also been found to correlate with mitochondrial and nuclear substitution rates.

Small-bodied organisms often have higher metabolic rates (when corrected for size) and may experience higher mutation rates due to the high concentration of free radicals in cells released as a by- product of oxidative metabolism (Gillooly et al. 2005; Gillooly and Allen 2007; Bromham 2011). Body size is widely known for being negatively correlated with population size (in general, small populations are associated with large body size) (Blackburn and Gaston 1999). However, the nearly neutral theory suggests a converse pattern with small populations experiencing a high fixation of nearly neutral mutations due to the increased influence of drift over selection, and thus exhibiting high substitution rates (Ohta 1972, 1973; Woolfit and Bromham 2003; Lanfear et al. 2013). Generation time and body size are generally positively correlated, with small-bodied species having shorter generation times, a greater number of germ cell division per unit time and, therefore, a higher mutation rate. The full extent to which these rate differences influence the topology of phylogenetic trees remains unclear, in part due to relatively low variation in body size and life history traits among study species.

The striking difference in body size among taxa may be one of the causes obscuring the true relationships among the main groups of Procellariiformes as a consequence of rate heterogeneity and related differences in branch lengths. Body size differences may cause striking differences in branch lengths that may ultimately lead to a series of artefacts, such as LBA (Felsenstein 1978) that, if not taken into account, can result in a phylogeny demonstrating inaccurate evolutionary relationships. In fact, molecular rate heterogeneity in the *cytochrome-b* gene related to body size was previously found to be present across the phylogeny of the Procellariiformes (Nunn and Stanley 1998). Additionally, other

factors such as ILS of ancestral variation and ancestral introgression may have contributed to the inconsistencies among procellariiform genealogical relationships.

### 1.4 Ultraconserved elements to study deep-evolutionary histories

Ultraconserved elements (UCEs) are genetic regions that are highly conserved across vertebrates and may be involved in fundamental stages during their development (Bejerano et al. 2004; Sandelin et al. 2004; Woolfe et al. 2005). Most UCE loci are located within non- coding regions, although some have been found to fall within exons. They are very conserved, even among species diverging as much as 300-400 million years ago, likely as a result of purifying selection (i.e. negative selection) (Bejerano et al. 2004; Katzman et al. 2007; Reneker et al. 2012). This very strong purifying selection is likely to occur due to their key regulatory role. Despite their highly conserved core, they become increasingly variable towards the flanking regions (Fig. 5; Faircloth et al. 2012). UCE cores together with their flanking regions range from 400 to 750 bp and are generally separated by more than 2 Mb. They are likely to segregate independently and are orthologous among many taxonomic groups (McCormack et al. 2011).While the conserved core allows capture and alignment of sequences from phylogenetically distant taxa, the variable sites are phylogenetically informative (Faircloth et al. 2012). Exons have been widely used in phylogenetics and despite their higher content of informative sites, UCEs show lower saturation scores which can help in deep-level inferences (>30 Ma) where homoplasy tends to be present and phylogenetic signal may be obscured (McCormack et al. 2011).

UCEs have been used to successfully resolve challenging deep-level relationships in turtles (Crawford et al. 2012), mammals (Mccormack et al. 2012), birds (McCormack et al. 2013; Manthey et al. 2016), formicine ants (Blaimer et al. 2015), fish (Longo et al. 2017) and bees (Bossert et al. 2019). UCEs have also been proven to be a good approach for inferring shallower relationships (population and species-level, <1 Ma) (Smith et al. 2013; Faircloth et al. 2015; Harvey et al. 2016).

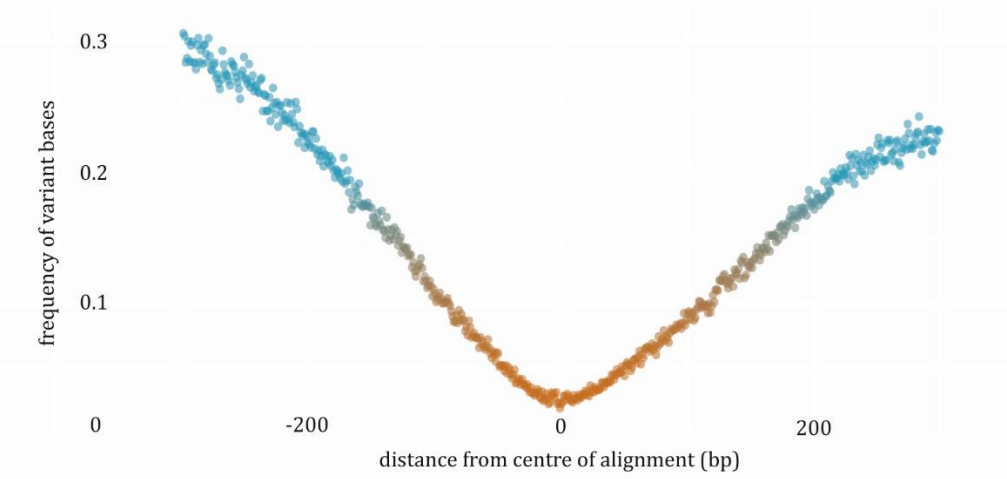


**Figure 5.** Nucleotide variability of our 4365 UCE dataset. The core regions (coloured in orange and based on the SWSC-EN results) have low frequencies of variable sites. Towards the flanking regions (blue), these elements become more variable.

### 1.5. Systematics

The pattern of evolutionary divergence of the four main groups of Procellariiformes has long been one of the unresolved questions in avian phylogenetics (Fig. 3). The best available estimates of the split between the main lineages puts it at around 30-35 Mya during the Eocene epoch (Feduccia and Mcpherson 1993; Prum et al. 2015). Four families are now usually recognised within this order: the albatrosses (Family Diomedeidae), the northern and southern storm- petrels (Families Hydrobatidae and Oceanitidae) and a very diverse group containing the gadfly petrels, fulmarines, prions and the diving-petrels (Family Procellariidae) (Warham 1990). However, the diving petrels (*Pelecanoides*) were long considered to constitute a separate family (Pelecanoididae) and this classification has received some molecular support (e.g., Sibley and Ahlquist 1990, Nunn and Stanley 1998). Conversely, the northern and southern storm-petrels were previously considered to belong to the same family (Hydrobatidae) and their monophyly is still debated (Sibley and Ahlquist 1990; Nunn and Stanley 1998; Kennedy and Page 2002) .

Genetic data, thus far, have not been able to elucidate the deeper evolutionary history of this order (Fig. 3). The phylogenetic study with the most comprehensive taxon sampling relied on a single mitochondrial marker – the *cytochrome-b* gene, and did not provide estimates of branch support (Nunn and Stanley 1998). Subsequent order-wide studies included taxon-poor datasets and small amounts of genetic data, sometimes

combined with morphological and behavioural traits (Kennedy and Page 2002; Penhallurick and Wink 2004; Mayr and Smith 2012).

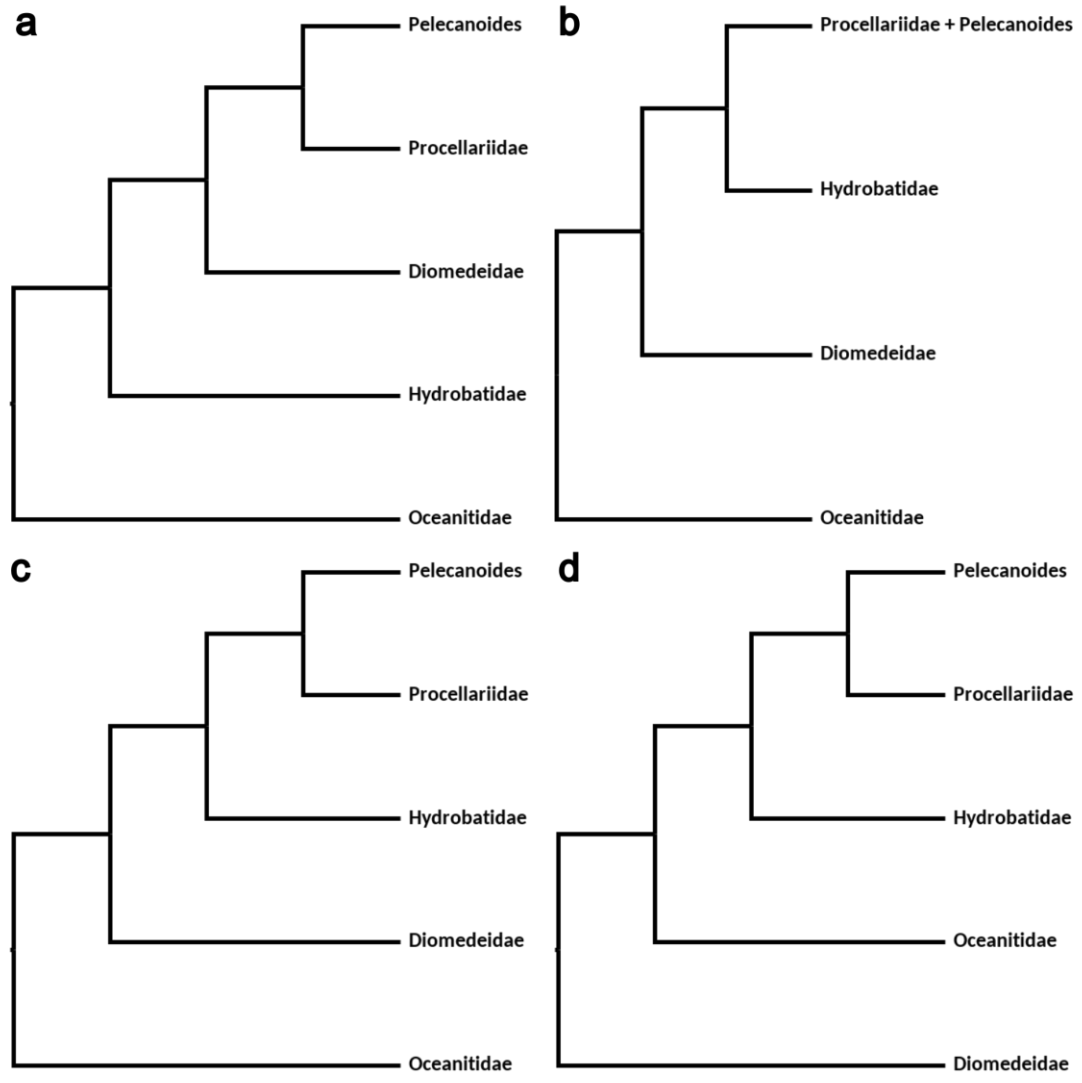


**Figure 3.** Most relevant published relationships among the main procellariiform lineages according to (a) Nunn and Stanley 1998 (*cytochrome-b*, 98 taxa) (b) Kennedy and Page 2002 (*cytochrome-b*, 122 species) (c) Hackett et al. 2008 (~32 kilobases of aligned nuclear DNA sequences, 5 procellariiform taxa) and (d) Prum et al. 2015 (259 nuclear loci, eight procellariiform taxa) and Reddy et al. 2017 (54 nuclear loci, six procellariiform taxa).

More recently, a number of studies using multiple genes or phylogenomic datasets of higher-level avian phylogenetics have included small numbers of species of Procellariiformes in their trees (Ericson et al. 2006; Hackett et al. 2008; Prum et al. 2015; Reddy et al. 2017). However, little can be concluded from these studies because of the paucity of representatives of this order that were included.

Reddy et al. (2017) thoroughly examined two Neoaves topologies: Jarvis et al. (2014) and Prum et al. (2015), which included some procellariiform representatives. They found that the type of datasets could lead to different topologies and that dense taxon sampling is not as important as long as the high level diversity is well represented. While Prum et al. (2015) included exhaustive and dense taxon sampling and used mainly coding regions (82.5% of the dataset was composed by exons), Jarvis et al. (2014) used introns, UCEs and exons. Reddy et al. (2017) highlights the importance of data type, remarking that non-coding regions are easier to model and they likely give a better representation of true evolutionary relationships. Despite this comment, Reddy et al. (2017) found the same procellariiform topology as Prum et al. (2015). Within the studies that analyse this order applying genome wide data, Hackett et al. (2008) is the most disparate genome-wide topology revealing the Oceanitidae family as the basal group (Fig. 3). This phylogeny was the result of 19 loci spanning 32 kb mainly across introns.

### 1.6 Aims

The goal of this thesis is to explore whether the presence of rate heterogeneity among Procellariiformes lineages biases the resulting topology. I evaluate whether body mass and a life-history trait (age first breeding, AFB) are correlated with substitution rate. This work also aims to unravel: (a) which procellariiform lineage is the basal group, (b) whether the storm petrels are monophyletic or paraphyletic and therefore separate families, (c) whether the diving petrels (genus *Pelecanoides*) are nestled within the Procellariidae. For this purposes, I will use sequences of 4,365 UCE loci from 51 species, representing all genera and all major lineages.

We expect to (1) find a robust topology using diverse phylogenetic inference methods (BI, ML, species tree methods) thanks to the vast genomic dataset that we have generated; (2) find extensive rate heterogeneity as Nunn and Stanley (1998) previously

found, with the albatrosses showing short branch lengths and the storm-petrels very long branches. (3) We hypothesise that body size and AFB are correlated with substitution rates and that they explain a substantial part of the rate variation. (4) We expect to recover a very similar phylogeny to previous studies using genome-wide data (with procellariiform sampling reduced to a single representative per family).

# CHAPTER II. MATERIALS AND METHODS

## 2.1 Taxon sampling

We assembled tissues from 51 individuals representing all major lineages within the order Procellariiformes (Supplementary Table S1). We additionally sequenced three species as outgroups: (i) an African penguin (*Spheniscus demersus*), (ii) a maguari stork (*Ciconia maguari*) and (iii) a brown booby (*Sula leucogaster*). Penguins (Sphenisciformes) are the sister group to Procellariiformes, and the storks and boobies represent somewhat distant groups (Prum et al. 2015).

All samples were requested from museums or collaborators after writing a small proposal justifying the destructive sampling of the requested tissue or skin.

## 2.2 Library preparation, targeted enrichment of UCEs and sequencing

We extracted genomic DNA from 0.5 g of tissue using Qiagen DNeasy Blood & Tissue Kits (Qiagen Inc., Valencia, CA, USA). We quantified all DNA extracts with a Qubit Fluorometer (Life Technologies, Inc.) using the high sensitivity kit and assessed DNA quality by gel electrophoresis. UCE capture and sequencing from our extracts was done by RAPiD Genomics. We used 100 bp paired-end Illumina Hiseq 2000 sequencing run and 16 cycles in both pre- and post-capture PCR reactions. (Gainesville, FL, USA). Each pool was enriched using custom-designed probes (MYbaits; MYcroarray, Inc., Ann Arbor, MI, USA) targeting 5,060 UCEs across tetrapods (Faircloth et al. 2012).

## 2.3 Assembly, alignment, trimming and data matrices

We evaluated the quality of the raw reads with FASTQC (Babraham Bioinformatics) and then removed Illumina adapter contamination and trimmed low-quality regions with the parallel wrapper script Illumiprocessor (https://github.com/fairclothlab/illumiprocessor). The PHYLUCE package v1.5.0 (Faircloth 2016; https://github.com/faircloth-lab/phyluce) was used for the initial sequence processing stages: We *de novo* assembled the reads into contigs with Trinity (*assemblo_trinity.py*) (Grabherr et al. 2013) and matched the assembled contigs to UCE probes (*match_contigs_to_loci.py*) (Faircloth et al. 2012). A list containing the UCE

loci enriched in each taxon was generated, we then created a FASTA file with data for each taxon and UCE locus (*get_fastas_from_match_counts.py*).

UCEs were aligned using MAFFT (Katoh et al. 2005, *phyluce_align_seqcap_align*) and the alignments were trimmed using a parallel wrapper around Gblocks (*phyluce_align_get_gblocks_trimmed_alignments_from_untrimmed*; Castresana 2000). Following alignment, we removed locus names (*remove_locus_name_from_nexus_lines.py*) and created three matrices with varying amounts of missing data (across taxa): 95%, 85% and 75% (*align_get_only_loci_with_min_taxa.py*). We calculated the number of informative sites for each alignment (*get_align_summary_data.py* and *get_informative_sites.py*) and evaluated their quality with the TriStats module within the TriFusion package, (http://odiogosilva.github.io/TriFusion/; Fischer et al. 2011). We generated PHYLIP- formatted, concatenated alignments based on our final data matrices (*format_nexus_files_for_raxml.py*) for phylogenetic analyses.

## 2.4 Phylogenetic analyses

### *2.4.1 Compositional bias*

We calculated the GC content and average base counts for each species and performed a chi-square test to identify potential base compositional bias, which if present can lead to inconsistent phylogenetic results (Supplementary Figure 1, Supplementary Table S2).

### *2.4.2 Model testing*

Two partitioning schemes were created. First, we utilised a locus partitioned scheme (partitioning scheme one), which uses each UCE as a separate partition with a potentially separate substitution model. Second, we employed an entropy-based partitioning scheme using SWSC-EN (partitioning scheme two; Tagliacollo and Lanfear 2018), which splits each UCE locus into 3 parts – the core and the two flanking regions, and allows different substitution models for each region of each UCE locus. We used the 75% matrix for most analyses because the alignment was the longest of the three matrices and the amount of missing data was still low. Due to computational demands, for the BI we were only able to use partitioning scheme one with the 95% matrix, which comprises a shorter alignment.

The resulting partitions from each analysis were used as input for PartitionFinder2, which finds the best partitioning schemes by lumping together those partitions that have similar substitution rates and selects the best-fitting substitution model for each subset (Lanfear et al. 2017). We linked the branch lengths and used a relaxed hierarchical clustering algorithm (rcluster method) with the –rcluster-max option set to 100. We only evaluated the models that RAxML can accommodate (GTR, GTR+G and GTR+I+G*) and selected the best scheme using the AIC with correction for small sample sizes (AICc). When the sample size is small the standard AIC tends to select models with too many parameters. For scheme one the total number of partitions was 1,696, while for scheme two it was 12,313.

* GTR = Generalised time reversible. GTR is the most neutral, independent and time-reversible substitution model. Base frequencies are variable and the substitution matrix symmetrical (e.g. Rodriguez et al. 1990). Gamma distribution (G) = Rate variation among sites is gamma distributed. Proportion of invariable sites (I) = Sites across the datasets are not allowed to change.

### *2.4.3 Maximum-likelihood analyses*

Maximum-likelihood (ML) phylogenetic analyses were performed with RAxML v8.0.19 (Stamatakis 2014). We used two different approaches: we performed a partitioned analysis (using scheme 2 described above) only for the 75% matrix and unpartitioned analyses for each of the matrices: 75%, 85% and 95%. Based on PartitionFinder2 results, GTR and GTR+G substitution models were the best fit models for most of the partitions, so for the unpartitioned analyses we ran two ML analyses under each of those two models for all three matrices and compared the resulting topologies. Bootstrap replicates were carried out using the autoMRE algorithm for each of the 100 independent ML searches. Results were visualised using Figtree v1.4.3 (http://tree.bio.ed.ac.uk/software/figtree/; Rambaut 2017).

We also ran IQ-TREE v.1.6. (Nguyen et al. 2015; http//:iqtree.org/) with our 75% matrix with partitioning scheme two. A GTR model with four General Heterogeneous evolution On a Single Topology (GHOST) linked classes, which account for heterotachous evolution (rate heterogeneity across sites) (Crotty 2017), was used.

*2.4.4 Bayesian analyses*

To estimate phylogenies in a Bayesian framework, we used Exabayes v1.5 (Aberer et al. 2014). We conducted unpartitioned analyses (75%, 85% and 95% matrices), with four independent runs each, using default priors and four coupled chains (three heated chains and one cold) for one million iterations and sampling every 500 generations. Convergence was assessed with Tracer v1.7.1 (Rambaut et al. 2018) by looking at the estimated sample sizes (EES) and checking the presence of a horizontal trend in traces of the likelihood across generations. All analyses converged and we applied a 10% burn-in to present consensus trees with PP support summarized from the marginal distribution of trees. Due to computational demands, the partitioned analysis was performed with only the 95% matrix and the locus partitioned scheme (scheme one above), and two independent runs for one million generations were carried out and a 25% burn-in applied.

*2.4.5 Species tree analyses*

In order to conduct species tree analyses, we first used RAxML v.8.0.19, to estimate gene trees for each of the 4,365 UCE loci, under a GTR+G substitution model. Species trees were calculated without multilocus bootstrapping in ASTRAL-III, as recommended by Sayyari and Mirarab (2016), who showed that internal branch support values are more reliable when bootstrapping is not performed. ASTRAL uses dynamic programming to search for the tree that shares the maximum number of quartet topologies with input gene trees (Zhang et al. 2018). Due to the high conservation of the UCE core, these markers can have a low number of informative sites. Following the protocol from Longo et al. (2017), we used the AMAS software (Borowiec 2016) to calculate the number of informative sites for each locus, selected the top 25% of loci that were most informative, and then repeated the same analysis as described above.

*2.4.6 Lineage-specific rate heterogeneity*

To investigate the effect of rate heterogeneity across the phylogeny, we tested two hypotheses: (i) the null model assumed that all lineages evolved under a constant rate of evolution, regardless of body size (i.e. a strict clock model) and (ii) an alternative model in which rates of evolution were allowed to vary among lineages (an uncorrelated lognormal relaxed clock model). Drummond et al. (2006) demonstrated that when rate

heterogeneity is present, uncorrelated models perform better than correlated models (Brown and Yang 2011).

We conducted two independent sets of analyses in BEAST v1.8.4 (Drummond et al. 2013). Since BEAST cannot handle alignments longer than 20,000 bp, we created 100 random datasets of our data by randomly selecting and concatenating UCE loci sequences so that the total length was between 19,000 and 20,000 bp. For each dataset we tested the fit of different substitution models – GTR, GTR+G, GTR+G+I, HKY+G, HKY+G+I and HKY – by calculating Bayes Factors (BFs). We ran an independent BEAST analysis for each dataset using the HKY substitution model. Tree topology and clock model were linked by locus and branch lengths were not, constraining topology and clock model but allowing branch length to vary across partitions. We applied a birth-death process (a special case of continuous-time Markov process. There are two types of transitions: "births" and "deaths". An increment of one on the state variable would be a "birth" while the decrease a "death"). We ran the analyses for 20 million iterations sampling every 20,000. All replicates converged in less than 20 million iterations with all parameters showing an ESS greater than 200. Log files were checked for convergence and adequate ESS with Tracer v1.7.1. We used Sumtrees v4.0.0 within the Dendropy v4.4.0 python package (Sukumaran and Holder 2010) to summarise all trees into a consensus tree using a Maximum Clade Credibility Topology (i.e. a topology that maximises the product of the clade PPs) and retained clades with a PP greater than 0.4. By calculating node heights of the relaxed clock tree in Figtree we obtained quantitative measures to compare rate heterogeneity between groups of taxa. The height of a node represents the distance of the longest path from a node to a tip.

Using a stepping stone/path sampling analysis (Leaché et al. 2014), marginal likelihood estimates (MLE) were calculated for each dataset using 10 million generations and sampling every 10,000 steps. Then we calculated each model MLE by combining all the dataset output files under each clock. MLE results allowed us to calculate the BFs and compare the best- fitting model. We calculated ln(BF) using the BF=2 x (model 1 - model 2) and evaluated the strength of the support using the Kass and Raftery (1995) framework.

*2.4.7 Phylogenetic comparative analyses*

We used phylogenetic comparative analyses to test whether body mass, AFB or the combination of both variables were correlated with substitution rate. We collected mass and AFB data from Brooke (2004), The Handbook of the Birds of the World (del Hoyo et al. 2014) and the primary literature (see Supplementary Table S3 and S4). When female and male mass was available we used the mean of both masses.

In order to carry out this correlational study while controlling for the phylogeny, we conducted PGLS analyses (Blomberg et al. 2012). Following the recommendations of Cooper et al. (2016), we first tested the assumptions of PGLS analyses, and then used the packages *ape*, *geiger*, *nlme* (Pinheiro et al. 2018) and *caper* (Orme 2013) to examine whether there were correlations among branch length and body size and AFB.

We used R 3.5.0 (R Core Team 2018) to carry out analyses of the correlation between body size, AFB and molecular rate. As a proxy for substitution rate, we collected data on the length of the branches of the partitioned Bayesian tree from Exabayes. We first removed all outgroups except the penguin by using the function *drop.tip* within the package *ape* (Paradis and Schliep 2018), and then we used the patristic option in the *distRoot* function within the package *adephylo* (Jombart et al. 2010) to measure the sum of branches from root to tip. We then removed all outgroups from the body mass and AFB data and calculated the log of the variables to normalise data for the PGLS analysis. Using the package *geiger* (Harmon et al. 2007), we explored the fit of two models of evolution (Brownian motion model and Ornstein-Uhlenbeck model) for each variable using the *fitContinuous* function. All plots were constructed using *ggplot2* (Wickham 2016).

# CHAPTER III. RESULTS

## 3.1 UCE sequence data

The mean number of UCE reads per sample was 1.98 million (Standard deviation (SD) = 80,536). We assembled reads into an average of 8,039.81 contigs per sample (SD = 138.75), from which we identified and recovered 4,926 UCE loci and a total of 2,521,401 bp. Individual UCE alignments had a mean length of 576.73 bp (Table 1; SD = 10.5). Missing data was very low in all matrices with values lower than 14% (Table 1, Supplementary Figures S1 – S6). GC content was homogeneous across taxa (Supplementary Table 2, Supplementary Figure 1, $\chi^2$=0.001, p-value=1.0).

| | **95% Matrix** | **85% Matrix** | **75% Matrix** |
|---|---|---|---|
| Min. taxa per locus | 51 | 45 | 40 |
| Alignment length (bp) | 1096476 | 2200911 | 2328288 |
| Missing data (%) | 5.88 | 13.34 | 10.64 |
| GC content (%) | 38.17 | 39.18 | 39.15 |
| Loci (n) | 1908 | 4048 | 4365 |
| Min length of UCE loci (bp) | 245 | 203 | 203 |
| Max length of UCE loci (bp) | 1205 | 1522 | 1522 |
| Mean length of UCE loci (bp) | 574 | 544 | 534 |
| 95% CI for mean length (bp) | 5.08 | 3.78 | 3.83 |

**Table 1.** Summary of the 95%, 85% and 75% data matrices (based on missing taxa). CI = confidence interval. Missing data refers to the final concatenated alignment for all taxa.

For most analyses we used the 75% matrix because it comprises the longest alignment (2,328,288 bp from 4,365 UCE loci) with still a low amount of missing data (10.64%). This matrix contained 294,892 variable sites (12.67%) and 141,901 informative sites (6.09%). The 95% matrix (1,096,476 bp) was exclusively used for the Bayesian partitioned analysis with partitioning scheme one because the length of the other alignments (2,200,911 bp and 2,328,288 bp) and the number of partitions meant that computational demands were too high for the other analyses.

### 3.2 Phylogenetic analyses

Partitioning scheme one, partitioned by locus, resulted in 1696 partitions. The best- fitting substitution model for all partitions was GTR+G+I, followed by GTR (Supplementary Table S5). The entropy-based partitioning analysis (SWSC-EN, partitioning scheme two) resulted in a highly partitioned alignment that identified 12,313 distinct data partitions. For half of the partitions the GTR substitution model fit best, and for the other half the GTR+G model was best. In our dataset, the cores evolved more frequently under a GTR substitution model and flanking regions under a GTR+G model (Supplementary Table S6,$\chi$2=157.71, p- value=0.00).

The topologies recovered from different tree building methods were essentially identical. All the RAxML results – 75%, 85%, 95% unpartitioned analyses implemented with both GTR and GTR+G substitution models, as well as the 75% partitioned (partitioning scheme two) – yielded the same fully resolved topology with all nodes supported with bootstrap values of 100 (Fig. 6). IQ-TREE yielded the same topology as well, though two nodes (the *Ardenna-Calonectris* node and the *Thalassoica-Daption* node) received 99% bootstrap support rather than 100 (Supplementary Figure S7). Trees from the BI analyses – 75% unpartitioned and 95% partitioned (partitioning scheme one) – show the same topology as the ML trees with all nodes showing PPs of 1.

In all analyses, the albatrosses (Diomedeidae) are sister to all other ingroup taxa, and the two groups of storm-petrels (Oceanitidae and Hydrobatidae) are each monophyletic but not sister to each other, thus confirming their paraphyly (Fig. 6). Finally, Procellariidae appears as the sister group of Hydrobatidae. Within the Procellariidae, the fulmarine petrels are sister to the rest of the group and the diving-petrels and prions form a monophyletic clade sister to the gadfly petrels. *Bulweria* and *Pseudobulweria* petrels are sisters and closely related to the shearwaters.

Branch lengths are comparatively long among both groups of small-bodied storm-petrels and short among the much larger albatrosses. However, the longest branch across the phylogeny is associated with the small-bodied diving-petrels (*Pelecanoides*), which are nestled within the Procellariidae.

We used two approaches for building species trees: we built gene trees for (i) every UCE locus in our complete dataset and (ii) the top 25% most informative UCE loci. Species trees were built from gene trees (see section *2.4.5 Species tree analyses*) applying both methods show the same topology as in the ML and BI trees (Supplementary Figure S8). The support values correspond to local PPs as described in Sayyari and Mirarab (2016).

As with other analyses, support was very high over most of the tree, although two nodes (the node uniting the three groups of shearwaters and the node uniting the diving petrels and the gadfly petrels) received slightly lower support (0.77 and 0.86 respectively).

### 3.3 Lineage-specific rate heterogeneity

To test the impact of among-lineage rate variation on the topology, we applied strict and uncorrelated relaxed clock models in BEAST for 100 randomly selected ~20,000 bp datasets of our data. From the consensus tree for the relaxed clock analyses we investigated differences in substitution rates. The node heights of albatrosses range from 0.59 to 0.61, the long branches of the diving petrels show heights of 0.04-0.11 and the storm-petrels 0.16-0.31 (Supplementary Figure S9). Note that Figtree scales node height from 1 to 0, being 1 the lowest height and 1 the maximum height possible. We found strong support (ln(BF) = 5.71) for the uncorrelated lognormal relaxed clock model (MLE = -42933) over the strict clock model (MLE = -43084), suggesting that different lineages in our topology experience different nucleotide substitution rates. The consensus tree resulting from the combination of the 100 datasets under both clock models is the same as the ML, BI and species trees topologies (Fig. 7).

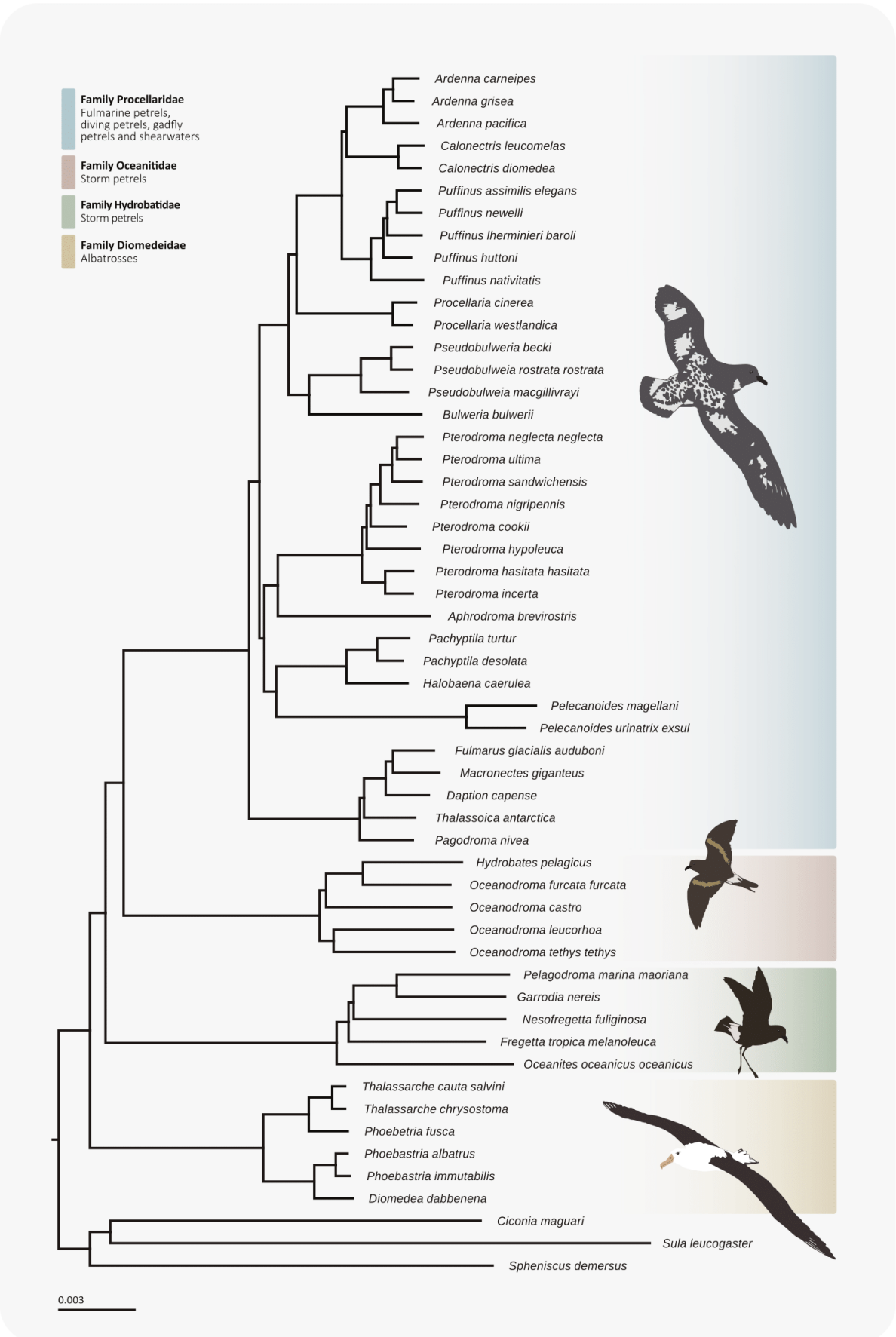


**Figure 6.** Best-fit phylogeny from the RAxML analysis of the partitioned 75% matrix under a GTR+G substitution model. All bootstrap support values = 100. All ML and Bayesian analyses lead to the same topology under different substitution models and different partitioning schemes.

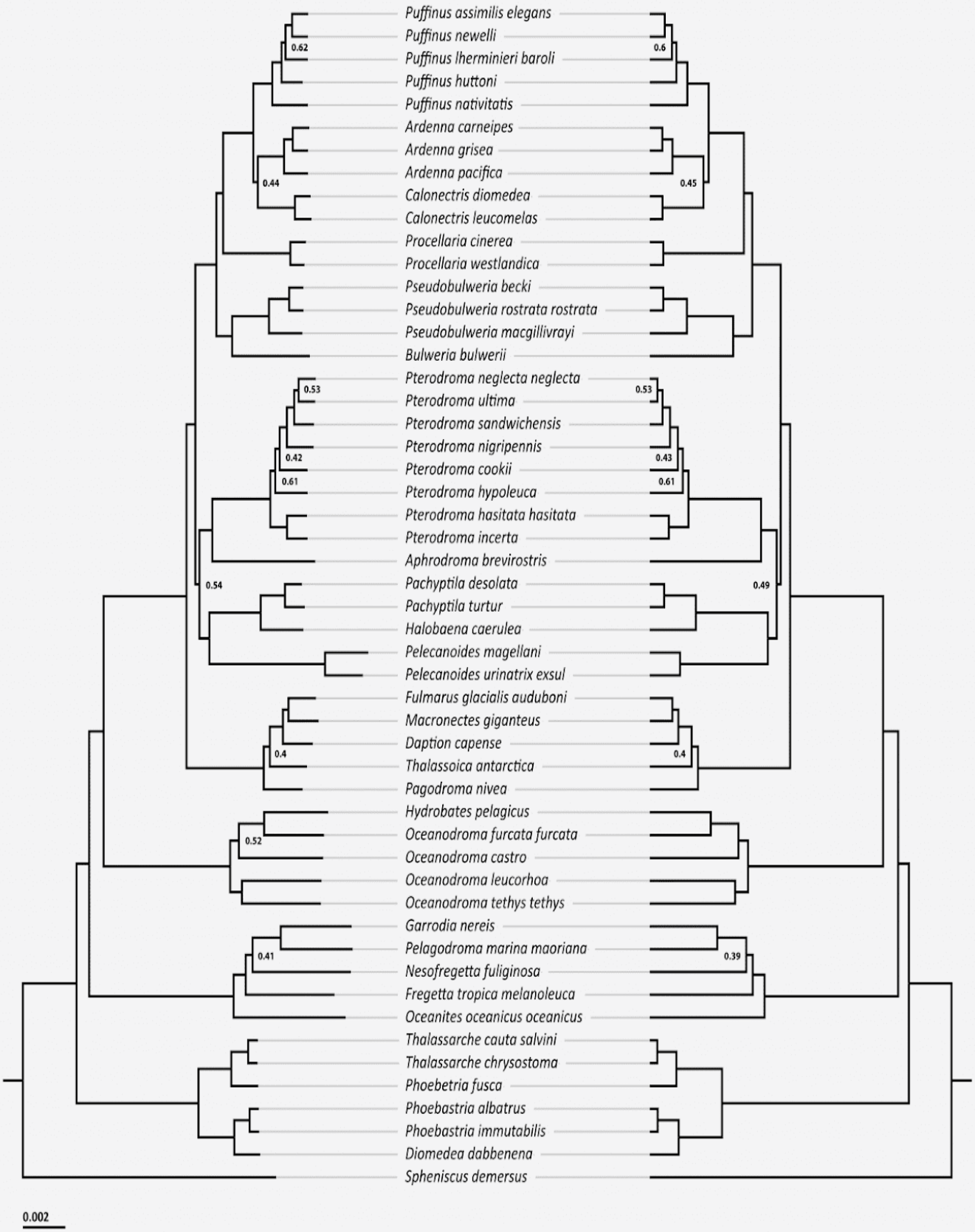


**Figure 7.** Comparison between the tree under a relaxed clock model (left) and a strict clock model (right). The topology remains the same, but note the differences in branch lengths. All nodes are supported by at least 0.7 unless otherwise indicated.

### 3.4 Body size, age at first breeding, and rate heterogeneity

Data on AFB are lacking for many seabird species, including 14 of the 51 species in our analysis, whereas body mass measurements are available for every species (Fig. 8, Table 2, Supplementary Tables S3, S4).

| Group | Body mass (g)±SD | Age at first breeding±SD | Node heights±SD | Samples (n) |
|---|---|---|---|---|
| Diomedeidae | 4309.17±1957.72 | 10.72± 1.69 | 0.6±0 | 6 |
| Oceanitidae | 48.02±13.91 | 4.10±0.80 | 0.3±0.01 | 5 |
| Hydrobatidae | 40.78±14.03 | 4.75±0.35 | 0.18±0.04 | 5 |
| Procellariidae | 400.36±251.36 | 6.93±2.44 | 0.37±0.02 | 32 |
| *Pelecanoides* | 157.95±5.73 | 2±0 | 0.1±0.01 | 2 |
| *Macronectes* | 4440±- | 11.4±- | 0.32±- | 1 |

**Table 2.** Average body mass and AFB of the main families and outliers within the Procellariiformes. See also Supplementary Tables S3-S4.

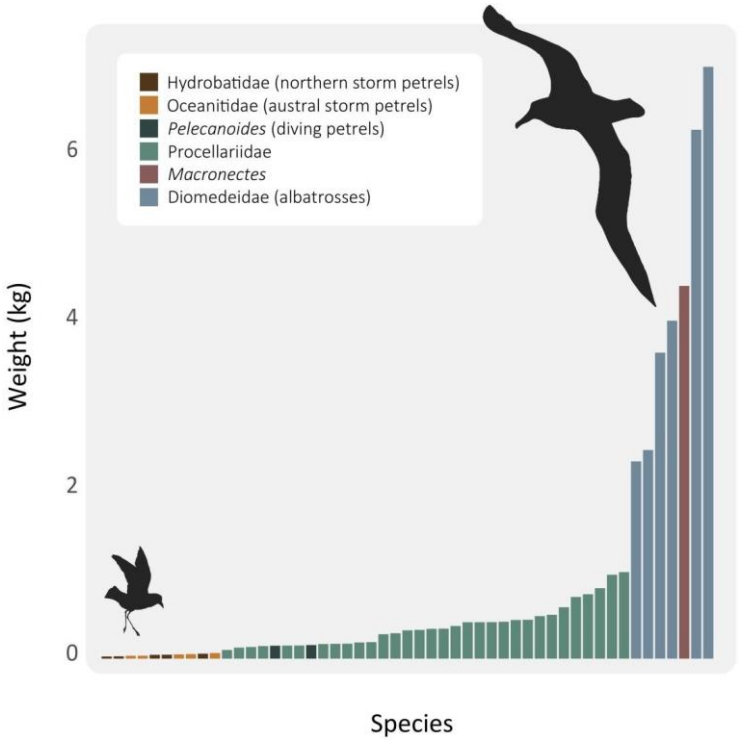


**Figure 8**. Mean mass by species within the order Procellariiformes. The albatrosses and *Macronectes* show the highest mass whereas the two groups of storm-petrels the lowest.

The body mass data demonstrates three clear clusters: (i) the albatrosses plus *Macronectes* (a large-bodied petrel from the Procellariidae family), (ii) the family Procellariidae, which comprises a very diverse group of birds, not only in genetic terms but also in many traits such as body size (see Fig. 9 and note the dispersion of the points in the Procellariidae cluster), and (iii) the two groups of storm-petrels, which cluster together, but can still be distinguished by phylogenetic group. The diving-petrels appear as a distinct cluster with very long branch lengths but a mass typical of the smaller species of Procellariidae. Age at first breeding show a similar trend (Supplementary Fig. 14).

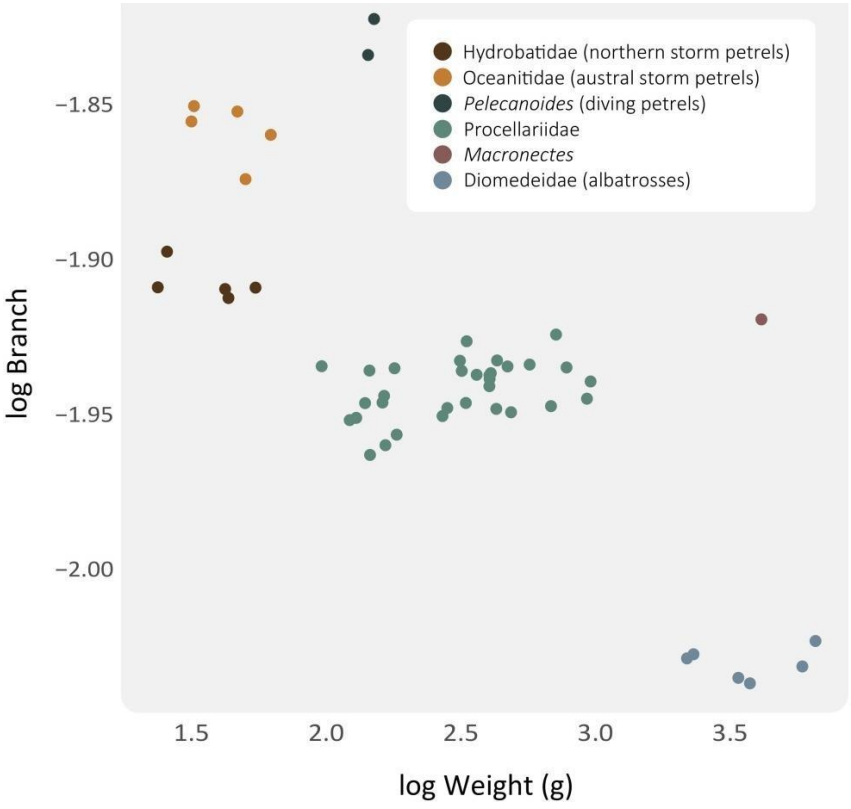


**Figure 9.** Relationship between body mass and branch length. Each family clusters together and is represented with a different colour. *Macronectes* and *Pelecanoides* are also represented by different colours as they are outliers.

Prior to performing the PGLS analysis, we tested the assumptions upon which PGLS is based, and found that, despite having three outliers for body mass (the two *Pelecanoides* species and *Macronectes*) and three outliers for AFB (two species of *Phoebastria* and *Thalassarche cauta salvini*), both body mass and AFB followed normal distributions. Plots of standardised contrasts and node heights did not reveal any outlier. Despite the presence of a few outliers, the studentised Breusch-Pagan test was

not significant, indicating that heteroscedasticity can be assumed and therefore PGLS assumptions are supported (Supplementary Figures S10- S12). In order to determine the best fitting model of evolution for PGLS analysis, AIC scores were calculated for the Brownian and the Ornstein-Uhlenbeck models. These models are based on similar assumptions and the scores were highly comparable (-104.814 and -104.55, respectively).

We first performed independent PGLS analyses for each of the two variables separately and then for the two together, and found that the model with two variables was best-fitting (R-squared=0.64; AIC = 60.27) (Table 3). The model with only AFB also performed well (AIC = 69.64, Supplementary figure S13), whereas the model with only body mass showed a higher AIC score (AIC = 108.75), indicating lower fit. We next removed a few outliers that were identified when we tested the assumptions of PGLS (see above), and carried out the analyses again. The model that performed best was also the one including both variables. The R-squared and AIC score for the model that included only weight without outliers improved, but the model with only AFB performed worse. The fact that the model including AFB performed better with outliers may be the result of too few data points and that those outliers fell not too far from the distribution. Overall and not surprisingly, the best-scoring model was the one including both variables without any outliers that deviated from the general trend within the rest of the order (R-squared= 0.72 and AIC = 53.95).

| | **R-squared** | **p-value** | **AIC** |
|---|---|---|---|
| Branch length ~ Body mass | 0.56 | 2.04E-10 | 108.75 |
| Branch length ~ AFB | 0.54 | 2.25E-07 | 69.64 |
| Branch length ~ Body mass + AFB | 0.64 | 1.77E-08 | 60.27 |
| Branch length ~ Body mass (no outliers) | 0.72 | 8.29E-15 | 60.04 |
| Branch length ~ AFB (no outliers) | 0.58 | 1.88E-07 | 78.72 |
| Branch length ~ Body mass + AFB (no outliers) | 0.72 | 7.53E-09 | 53.95 |

**Table 3.** PGLS output with branch as the dependent variable and body mass, AFB or both variables together as independent variables.

# CHAPTER IV. DISCUSSION

## 4.1 Genome-wide data and phylogeny

With 4,356 loci and a concatenated alignment length of 2.3 million bp, our study is among the largest phylogenetic datasets investigating a single order, in this case the avian order Procellariiformes. Our results suggest that, in the absence of other systematic biases, the use of large genome-wide datasets can mitigate the misleading effects of extensive among-lineage rate heterogeneity giving the best confidence in extracting true evolutionary relationships. All tree building methods used, and whether employing variable or constant rates, produced the same robust topology. The relaxed clock phylogeny shows lower PP values at some nodes compared to the support values of the ML and Bayesian analyses. This may be due to reducing the data for BEAST. The subsetting resulted in, at least, a 110 times reduction of our dataset (from 2.3 million bp to 20,000bp and approximately 35 loci per dataset). However, despite somewhat lower support values at some nodes, the main topology (ML, Bayesian and species tree topologies) was still recovered from the BEAST runs.

## 4.2 Shedding light on the procellariiform deep-evolutionary relationships

The largest Procellariiform phylogeny by Nunn and Stanley (1998) only included a single mitochondrial locus (*cytochrome-b*) and was based on a MP analysis without any measures of support. This and similar studies aimed to build a taxon-rich procellariiform phylogeny, but employed a small amount of mitochondrial sequence data and recovered disparate topologies with low support values at deep nodes (Kennedy et al. 2002; Penhallurick and Wink 2004). Other studies applied genome-wide data to address the evolutionary history of birds but included only one or a few representatives of each family (e.g. Prum et al. 2015; Reddy et al. 2017). Our strongly supported topology is in agreement with the latter studies although we provide much greater resolution (51 vs. 8 taxa) by sequencing representatives of all genera and at least five species from each family. Our results strongly support a single topology, with (i) the albatrosses (Diomedeidae) as the basal group, (ii) the two families of storm-petrels (Hydrobatidae, Oceanitidae) not sister to each other, (iii) the family Hydrobatidae as sister taxa to the Procellariidae, and (iv) the diving-petrels (*Pelecanoides*) placed within the Procellariidae.

Reconstructing deep-level evolutionary relationships can present several difficulties, including the presence of short internal branches indicative of periods of rapid divergence (e.g. Alda et al. 2018). This phenomenon can cause ILS, which may lead to the loss of phylogenetic signal at deep nodes and result in conflicting topologies (Rokas and Carroll 2006; Whitfield and Lockhart 2007; Wiens et al. 2008; Philippe et al. 2011; McCormack et al. 2013; Suh et al. 2015). Concatenation-based methods can be less accurate than coalescent- based approaches in the presence of ILS (e.g. Edwards et al. 2007; Bayzid and Warnow 2013). Here, we use the summary method ASTRAL-III which is statistically consistent under the multi-species coalescent. Our ASTRAL species trees show the same topology as in the ML and Bayesian analyses, although with somewhat lower support in some nodes, such as the node uniting the three species of *Ardenna* and the two species of *Calonectris* shearwaters, where support is 0.78 in the species tree compared to full support in the ML and Bayesian trees (Supplementary Figure S8 and Fig. 6). The short internal branches suggest that the shearwaters may have experienced rapid divergence, and that taxon-rich sampling combined with genome-wide markers may be needed to resolve their evolutionary relationships.

Another example of differing support values between different methods (ML, BI and species trees) is the relationship between the gadfly petrels and the group comprising the prions and the diving petrels (*Pelecanoides*). This relationship is supported by bootstrap values of 100 or PPs of 1 in the ML and Bayesian analyses, respectively. However, in the species tree the relationship is supported by a value of 0.86, which far from representing low support, it is relatively lower if compared with the rest of the values across the tree. This value and the short branch preceding the node may indicate that the 3 clades (prions-diving- petrels, shearwaters-*Bulweria*-*Procellaria* and *Pterodroma*) probably appeared as the product of a radiation within a short time period. Here it is likely that the internal short branch that unites these lineages has also led to incorrect inferences when using a small amount of genetic data, as applied in previous studies that suggested the *Pelecanoides* were placed outside the Procellariidae as a separate family.

### 4.3 Molecular rate heterogeneity

Systematic or non-random errors (e.g. gene-tree discordance, LBA, compositional and rate heterogeneity) are well-known problems in phylogenetics that appear with increasing dataset size (Felsenstein 1978). Given the striking differences in body size between albatrosses, the largest species of Procellariiformes, and the storm-petrels, the smallest (Fig. 2), we hypothesised that rate heterogeneity would be present among lineages.

Our ML and Bayesian trees support the hypothesis that there is rate heterogeneity across the procellariiform phylogeny. Clear differences in branch lengths occur between the albatrosses, which are large-bodied and expected to have slow substitution rates, and the storm-petrels, which are much smaller and have comparatively long branches. The pattern is also evident within the family Procellariidae, for example, in which the small *Pelecanoides* diving petrels exhibit comparatively long branches (Fig. 6 and 7, Supplementary figure S14). The relaxed clock analyses demonstrated highly supported differences in substitution rate between large-bodied (albatrosses) and small-bodied (storm-petrels and diving petrels) taxa, rejecting the clock-like evolution hypothesis at this taxonomic level, as previously suggested by Nunn and Stanley 1998. These results are in accordance with previous studies of a range of other taxa (birds: Pereira and Baker 2006; Patane et al. 2009; Pacheco et al. 2011; birds and reptiles: Eo and DeWoody 2010; plants: Beaulieu et al. 2015). All of these studies find disparate rates of substitution rate among the groups included in their studies, most of which analyse groups at the family-level.

### 4.4 Phylogenetic comparative tests on body size effects and molecular rate

While body size is an obvious candidate potentially driving differences in molecular rates, other related factors may be involved, such as population size and generation time. Body size has been proven to be highly correlated with metabolic rate in birds (Nagy 2005) and in sub-Antarctic species of Procellariiformes (Brown and Adams 1984), so we used adult body mass as a proxy for metabolic rate. Information about population size and generation time of this order of seabirds is extremely difficult to collect because most birds breed on remote islands and the recovery rate of bands is usually very low (e.g. Menkhorst 1984). We collected data on AFB with only 37 data points out of 51 species. This amount of missing data could have affected to the PGLS results, making the analysis

weaker. Adding more data points would increase the statistical power and could potentially lead to more trustworthy results.

We used branch lengths as a proxy for substitution rate by measuring the distance from root to tip. This method has been criticised because of the assumption that data points are phylogenetically independent when actually sampled sequences are linked by their evolutionary history (Drummond et al. 2003).

Other metrics could not be used as a proxy for substitution rate (e.g. dn/ds) as most of UCEs are non-coding DNA regions. However, Tong et al. 2018 compared the performance of regression of root to tip distances, least-squares dating and Bayesian inference on calculating substitution rate and found all of them to be consistent. Nunn and Stanley (1998) compared the terminal branches of sister taxa, but with our sampling scheme this would have resulted in just 15 comparisons in the case of mass and 12 in the case of AFB, thus suffering from low power. Also, the differences in terminal branch lengths are notable among groups and not within them. Coevol (Lartillot and Poujol, 2011) models substitution rates as Brownian diffusion processes in a Bayesian Monte Carlo framework. This software would have been useful but it requires fossil calibrations which are not yet available for this order. Our future work will aim to get calibration points across the tree and use this program to investigate the relative contribution of life history traits and body size to substitution rate.

Species of *Macronectes* are well-known for being the most sexually dimorphic of all seabirds (van Franeker and ter Braak 1993; Gonzalez-Solis et al. 2000; Copello et al. 2006) and indeed male and female *M. giganteus* differed substantially in body mass (4930g vs 3950g, respectively). However, female mass also well exceeded the Procellariidae mean and the AFB is substantially later (Table 3). According to our overall conclusions we should see a very short branch if compared to their closest relatives due to their high body mass and long generation time. However, the branch leading to *Macronectes* is within the values observed for other Procellariidae possibly due to its shared evolutionary history with the rest of species of this clade (see Supplementary Figure S14). On the other hand, the diving-petrels also stand out within the Procellariidae. Diving-petrels show very long branches, and their body sizes and generation times seem to be storm-petrel-like. In spite of being an outlier, phylogenetically speaking, this result follows the overall trend of small organisms with short generation times resulting in long branches. AFB follows the same trend as body mass. However, here *Macronectes* is no longer an outlier as more species of Procellariidae (e.g., species of *Procellaria*) breed as

late as the albatrosses (Supplementary Figure S13). The diving petrels also appear as a distinct group again, and are more similar to the two groups of storm-petrels.

PGLS results reveal a high correlation between branch length and body mass and life- history traits (in our case, AFB) as suggested in previous studies carried out using a wide range of organisms as well as those focusing specifically on birds (Jarvis et al. 2014; Weber et al. 2014; Berv and Field 2018). Our correlation coefficients are similar to those of Nunn and Stanley (1998) (AFB-Branch: $r^2$=0.458, Mass-Branch estimates missing), although our study covers more data points and result in a slightly higher correlation coefficient. According to our results, 64% of the variance in branch length is explained by the body mass and AFB. Adding more taxa and obtaining more data on AFB could further increase this correlation.

.

# CHAPTER V. SYNTHESIS

In this study, I investigated the presence of rate heterogeneity in a genome-wide dataset at the order level, and applied different clock models to examine the resulting impact on the topology recovered. The findings support substitution rate variation across lineages, rejecting the clock-like evolution hypothesis. I find that with a large genomic dataset, potential effects of rate heterogeneity can be avoided. I explored these questions with a dataset composed by UCEs. I also tested whether a life-history trait (AFB) and body mass are potential candidates driving rate heterogeneity and found a strong correlation between these variables and branch length, used as a proxy for nucleotide substitution rate. Genetic data only provide a relative timescale and one must know the absolute age of a divergence event in order to calibrate the molecular clock and estimate substitution rate (Donoghue and Yang 2016). For this purpose, we would have needed a few fossil calibrations which are not yet available for this order. Our future study will include fossil calibrations, which will not only provide substitution rates, but also a time-calibrated phylogeny.

For addressing these fundamental questions in phylogenetics I used a group of seabirds for which the evolutionary relationships have been unclear and strongly debated over the last two decades. I shed light on the deep relationships within the order Procellariiformes, providing a robust topology using multiple tree construction approaches. I corroborate that the backbone topology for the order Procellariiformes is essentially the same as the ones found using genomic data (Prum et al. 2017; Reddy et al. 2015). We find the albatrosses as the most distant group, the two groups of storm-petrels being paraphyletic and the diving petrels nestled within the Procellariidae.

## 5.1 Biases in phylogenetic inference

The accuracy of the different inference methods is a central debate in phylogenetics and thus knowledge of biases is large and increasing each year. Despite the amount of literature proposing hypotheses about the factors driving substitution rates, few studies have tested how among-lineage rate heterogeneity may impact tree topologies. To further explore this issue, it would be interesting to see the impact of other genome-wide datasets such as Anchored Hybrid Enrichment or Rapidly Evolving Long

Exons (RELEC) (Karin et al. 2019) to see if data types with other characteristics reveal inconsistencies in the resultant topologies.

Another interesting study would be getting datasets from species, family, order and class and make a comparative analysis to see at which taxonomic scale rate heterogeneity starts to be noticed. Rate heterogeneity is likely to be variable across taxonomic scales because they represent different levels of divergence. It is possible that rate heterogeneity is not as present in closely related species and more divergent species are likely to evolve different strategies and life history traits that will result in more extensive rate heterogeneity.

### 5.2 The evolution of body size in Procellariiformes

The plot for wing length by species reveals a gap between large-bodied and small-bodied procellariform species with a striking scarcity of procellariiform species of 40-50 cm of wingspan (Brooke 2004). Fossils of medium-size albatrosses (but larger than the Procellariidae) have been found in France and California (Olson 1985), but there are not many published hypotheses trying to explain this distribution. Studies in other organisms have suggested that intermediate-sizes species may be poor competitors against larger species (Kelt and Meyer 2009). As many other taxonomic groups, Procellariiformes shows a right skewed distribution of body sizes, which means that the frequency of small-bodied species is higher, probably because small species tend to be more specialised (Hutchinson and MacArthur 1959), although hypotheses relating energy efficiency to body size have also been proposed (Brown et al. 1993).

*Macronectes* (also known as the giant petrels) is an interesting exception within the Procellariidae because most members of this family are medium or small-bodied. This genus comprises two species characterised for being strikingly big. The two species overlap in their distribution which is restricted to high latitudes of the south hemisphere. It would be easy to think that the evolution towards a big body is a consequence of their distribution following Bergman's rule: larger-bodied species have smaller surface-area-to-volume ratios thereby increasing heat conservation in colder climates. This rule remains controversial (James 1970; Blackburn et al. 1999; Meiri and Dayan 2003, but see the discussion in Olson et al. 2009) and there are many other hypotheses trying to explain why big-bodied species tend to occur in high latitudes: higher resource availability (Rosenzweig 1968), better tolerance to seasonality and environmental fluctuations (Boyce 1978; Geist 1987), resistance to cold climates (Calder 1974; Zeveloff and Boyce

1988) and predator avoidance (Brown 1995). Most of the giant petrels' closest relatives share distribution with them but are small-bodied (e.g. many species within the genus *Fulmarus, Daption capense, Thalassoica antarctica* and *Pagodroma nivea* (the latter three are the only species in their respective genus)), so it is likely that in this particular case the evolution of a big body in giant petrels is the consequence of the adaptation to a particular environment and it would be necessary to examine all the candidate environmental and ecological drivers.

### 5.3 Future questions in procellariiform phylogenetics

Future studies aiming to fully resolve the procellariiform phylogeny at the species and subspecies-level will benefit from the backbone phylogeny proposed in this study. A well-resolved phylogeny will help in conservation management because the boundaries among these birds are often unclear (Friesen 2015). Cryptic speciation is a common phenomenon in this group of birds (Brooke 2004; Friesen 2015; Taylor 2017; Taylor et al. 2019), meaning that despite being morphologically indistinguishable, they are genetically distinct. In a normal scenario, hybridisation is avoided by a wide range of isolating mechanisms which in the case of Procellariiformes might be call differences or different patterns of plumage colour. However, because they are highly philopatric and dispersal is very low, admixture rarely occurs between birds of different species. Selection promoting phenotypic diversity is low among birds with even slightly different dispersal tendencies resulting in phenotypic homogeneity while having genetically divergent populations (Saastamoinen et al. 2017). Populations of gadfly petrels or albatrosses that are currently declining in numbers may consist of two genetically differentiated populations that do not interbreed but if conservation strategies are planned as if they belong to a single population, the number of breeding pairs would be overestimated and the threat would be much higher. The black-capped petrel (*Pterodroma hasitata*) is one potential example of cryptic speciation that has shown a great decline in the number of breeding pairs during the last few decades. Learning their true phylogenetic relationships to the species and subspecies level would help to improve their conservation strategy (Jose et al. 2009; Harris et al. 2012).

This backbone phylogeny could also be used to study trait evolution. Studying trait evolution of endangered seabird species may help to understand whether particular characteristics, such as nesting habitat and type, longevity, and foraging ecology (e.g. plunge diving, feeding near shore) are associated with extinction risk.

Most phylogenetic comparative methods assume that diversification rates are constant over time, and that older clades and those with higher diversification rates should have more species. However, ecological processes may cause diversity to reach a 'carrying capacity' and level off such that species richness is no longer directly related to time. Procellariiformes offer an ideal group of organisms in which to test these hypotheses because diversity levels and rates of molecular evolution are not constant across families, which indicate that rates of diversification may also be heterogeneous.

There are still many unanswered questions in avian phylogenetics. However, our results highlight the branching pattern of the main lineages within the Procellariiformes, setting a background that will allow researchers to further address questions related to their evolution, ecology and conservation.

## REFERENCES


Aberer A.J., Kobert K., Stamatakis A. 2014. ExaBayes: massively parallel Bayesian tree inference for the whole-genome era. Mol. Biol. Evol. 31:2553–2556.

Alda F., Tagliacollo V.A., Bernt M.J., Waltz B.T., Ludt W.B., Faircloth B.C., Alfaro M.E., Albert J.S., Chakrabarty P. 2018. Resolving deep nodes in an ancient radiation of Neotropical fishes in the presence of conflicting signals from incomplete lineage sorting. Syst. Biol. 0(0):1–21

Anderson F.E., Swofford D.L. 2004. Should we be worried about long-branch attraction in real data sets? Investigations using metazoan 18S rDNA. Mol. Phylogenet. Evol. 33:440–451.

Bayzid M.S., Warnow T. 2013. Naive binningimproves phylogenomic analyses. Bioinformatics. 29:2277–2284.

Beaulieu J.M., O'Meara B.C., Crane P., Donoghue M.J. 2015. Heterogeneous rates of molecular evolution and diversification could explain the triassic age estimate for angiosperms. Syst. Biol. 64:869–878.

Bejerano G., Pheasant M., Makunin I., Stephen S., Kent W., Mattick J., Haussler D. 2004. Ultraconserved elements in the human genome. Science. 304:1321.

Berv J.S., Field D.J. 2018. Genomic signature of an avian Lilliput Effect across the K-Pg extinction. Syst. Biol. 67:1–13.

Blackburn T.M., Gaston K.J. 1999. The Relationship between animal abundance and body size: a review of the mechanisms. Adv. Ecol. Res. 28:181–210.

Blackburn T.M., Gaston K.J., Loder N. 1999. Geographic gradients in body size: a clarification of Bergmann's rule. Divers. Distrib. 5:165-174.

Blaimer B.B., Brady S.G., Schultz T.R., Lloyd M.W., Fisher B.L., Ward P.S. 2015. Phylogenomic methods outperform traditional multi-locus approaches in resolving deep evolutionary history: A case study of formicine ants. BMC Evol. Biol. 15:1–14.

Blomberg S.P., Lefevre J.G., Wells J.A., Waterhouse M. 2012. Independent contrasts and PGLS regression estimators are equivalent. Syst. Biol. 61:382–391.

Bonadonna, F., Cunningham, G.B., Jouventin, P, Hesters, F., Nevitt, G.A. 2003. Evidence for nest-odour recognition in two species of diving petrel. J Exp Biol. 206: 3719–3722.

Borrelle S.B., Boersch-Supan P.H., Gaskin C.P., Towns, D. R. 2016. Influences on recovery of seabirds on islands where invasive predators have been eradicated, with a focus on Procellariiformes. Oryx,52:346-358.

Borrelle S.B., Buxton R.T., Jones H.P., Towns, D.R. 2015. A GIS-based decision-making approach for prioritizing seabird management following predator eradication. *Restoration Ecology*, *23*:580-587.

Borowiec M.L. 2016. AMAS: a fast tool for alignment manipulation and computing of summary statistics. PeerJ. 4:e1660.

Bossert S., Murray E.A., Almeida E.A.B., Brady S.G., Blaimer B.B., Danforth B.N. 2019. Combining transcriptomes and ultraconserved elements to illuminate the phylogeny of Apidae. Mol. Phylogenet. Evol. 130:121–131.

Boyce M.S. 1978. Climatic variability and body size variation in the muskrats (Ondatra zibethiens) of North America. Oecologia. 36:1-19.

Bromham L. 2002. Molecular clocks in reptiles: life history influences rate of molecular evolution. Mol. Biol. Evol. 19:302–309.

Bromham L. 2011. The genome as a life-history character: Why rate of molecular evolution varies between mammal species. Philos. Trans. R. Soc. B Biol. Sci. 366:2503–2513.
Brooke M. 2004. Albatrosses and Petrels across the World. Oxford University Press.
Brown C.R., Adams N.J. 1984. Basal Metabolic Rate and Energy Expenditure during Incubation in the Wandering Albatross (Diomedea exulans). Condor. 86:182–186.
Brown J.H., Marquet P.A., Taper, M.L. 1993. Evolution of body size: consequences of an energetic definition of fitness. Am. Nat. 154:573-584.
Brown J.H. 1995. Macroecology. University of Chicago Press, Chicago, Illinois, USA.
Brown R.P., Yang Z. 2011. Rate variation and estimation of divergence times using strict and relaxed clocks. BMC Evol. Biol. 11.
Calder W.A. 1974. Consequences of body size for avian energetics. Avian energetics. Nuttall Ornithological Club, Cambridge, Massachusetts, USA.
Castresana J. 2000. Selection of conserved blocks from multiple alignments for their use in phylogenetic analysis. Mol. Biol. Evol. 17:540–522.
Chor B., Tuller T. 2005. Maximum likelihood of evolutionary trees: hardness and approximation. Bioinformatics, 21:97-106.
Copello S., Quintana F., Somoza G. 2006. Sex determination and sexual size-dimorphism in Southern Giant-Petrels (Macronectes giganteus) from Patagonia, Argentina. Emu. 106:141–146.
Crawford N.G., Faircloth B.C., McCormack J.E., Brumfield R.T., Winker K., Glenn T.C. 2012. More than 1000 ultraconserved elements provide evidence that turtles are the sister group of archosaurs. Biol. Lett. 8:783–786.
Criscuolo A., Berry V., Douzery E., Gascuel O. 2006. SDM: A fast distance-based approach for (super)tree building in phylogenomics. Syst. Biol. 55:740–755.
Crotty S.M. 2017. GHOST : A time-reversible mixture model for recovering phylogenetic signal from heterotachously-evolved sequence alignments. Doctoral thesis.
Croxall J., Butchart S., Lascelles B., Stattersfield A., Sullivan B., Symes A., Taylor P. 2012. Seabird conservation status, threats and priority actions: a global assessment.
Drummond A., Pybus O.G., Rambaut A. 2003. Inference of viral evolutionary rates from molecular sequences. Adv. Parasitol. 54:331–358.
Drummond A.J., Ho S.Y.W., Phillips M.J., Rambaut A. 2006. Relaxed phylogenetics and dating with confidence. PLoS Biol. 4:699–710.Drummond A.J., Rambaut A. 2007 BEAST: bayesian evolutionary analysis by sampling trees. BMC Evol. Biol. 7:214.
Donoghue P.C., Yang Z. 2016. The evolution of methods for establishing evolutionary timescales. Philos. Trans. Royal Soc. B, 371:20160020.
Dornburg A., Townsend J.P., Friedman M., Near T.J. 2014. Phylogenetic informativeness reconciles ray-finned fish molecular divergence times. BMC evolutionary biology, 14:169.
Douglas H.D., Fernandez P. 1997. A longevity record for the waved albatross (Registro de longevidad para un individuo de Diomedea irroriata). J. Field Ornithol. 224-227.
Edwards S.V., Liu L., Pearl D.K. 2007. High-resolution species trees without concatenation. Proc. Natl. Acad. Sci. 104:5936–5941.
Ericson P. G., Anderson C. L., Britton T., Elzanowski A., Johansson U. S., Källersjö M., Ohlson J.I., Parsons T.J., Zuccon D., Mayr G. 2006. Diversification of Neoaves: integration of molecular sequence data and fossils. Biology letters, 2:543-547.
Eo S.H., DeWoody J.A. 2010. Evolutionary rates of mitochondrial genomes correspond to diversification rates and to contemporary species richness in birds and reptiles. Proc. R. Soc. B Biol. Sci. 277:3587–3592.

Faircloth B.C. 2016. PHYLUCE is a software package for the analysis of conserved genomic loci. Bioinformatics. 32:786–788.

Faircloth B.C., McCormack J.E., Crawford N.G., Harvey M.G., Brumfield R.T., Glenn T.C. 2012. Ultraconserved elements anchor thousands of genetic markers spanning multiple evolutionary timescales. Syst. Biol. 61:717–726.

Felsenstein J. 1978. Cases in which parsimony or compatibility methods will be positively misleading. Syst. Zool. 27:401–410.

Field D.J., Berv J.S., Hsiang A.Y., Lanfear R., Landis M.J., Dornburg A. 2019. Timing the extant avian radiation: The rise of modern birds, and the importance of modeling molecular rate variation. PeerJ Prepr.

Fischer S., Brunk B.P., Chen F., Gao X., Harb O.S., Iodice J.B., Shanmugam D., Roos D.S., Stoeckert C.J. 2011. Using OrthoMCL to assign proteins to OrthoMCL-DB groups or to cluster proteomes into new ortholog groups. Curr. Protoc. Bioinforma. 1:1–19.

van Franeker J.A., ter Braak C.T.. 1993. A generalized discriminant for sexing Fulmarine petrels from external measurements. Auk. 110:492–502.

Friesen V. L. 2015. Speciation in seabirds: why are there so many species… and why aren't there more? J. Ornithol, 156:27-39.

Geist V. 1987. Bergmann's rule is invalid. Can. J. Zool. 65:1035-1038.

Gillooly J.F., Allen A.P. 2007. Linking global patterns in biodiversity to evolutionary dynamics using metabolic theory. Ecology. 88:1890–1894.

Gillooly J.F., Allen A.P., West G.B., Brown J.H. 2005. The rate of DNA evolution: Effects of body size and temperature on the molecular clock. Proc. Natl. Acad. Sci. 102:140–145.

Gonzalez-Solis J., Croxall J., Wood A. 2000. Sexual dimorphism and sexual segregation in foraging strategies of northern giant petrels, Macronectes halli, during incubation. Oikos. 90:390–398.

Grabherr M.G., Haas B.J., Yassour M., Levin J.Z., Thompson D.A., Amit I., Adiconis X., Fan L., Raychowdhury R., Zeng Q., Chen Z., Mauceli E., Hacohen N., Gnirke A., Rhind N., Palma F. di, W. B. 2013. Trinity: reconstructing a full-length transcriptome without a genome from RNA-Seq data. Nat. Biotechnol.29:644–652.

Hackett S.J., Kimball R.T., Reddy S., Bowie R.C.K., Braun E.L., Braun M.J., Chojnowski J.L., Cox W.A., Han K., Harshman J., Huddleston C.J., Marks B.D., Miglia K.J., Moore W.S., Sheldon F.H., Steadman D.W., Witt C.C., Yuri T. 2008. A phylogenomic study of birds reveals their evolutionary history. Science (80-. ). 320:1763–1767.

Harmon L.J., Weir J.T., Brock C.D., Glor R.E., Challenger W. 2007. GEIGER: investigating evolutionary radiations. Bioinformatics. 24:129–131.

Hedges S.B., Marin J., Suleski M., Paymer M., Kumar S. 2015. Tree of life reveals clock-like speciation and diversification. Mol. Biol. Evol. 32:835–845.

Hendy M.D., Penny D. 1989. A framework for the quantitative study of evolutionary trees. Syst. Zool. 38:297–309.

Ho S.Y. 2014. The changing face of the molecular evolutionary clock. Trends in ecology & evolution, 29:496-503.

Hua X., Cowman P., Warren D., Bromham L. 2015. Longevity is linked to mitochondrial mutation rates in rockfish: A test using poisson regression. Mol. Biol. Evol. 32:2633–2645.

Huelsenbeck J.P., Ronquist, F. 2001. MRBAYES: Bayesian inference of phylogenetic trees. Bioinformatics. 17:754-755.

Hutchinson G.E., MacArthur R.H. 1959. A theoretical ecological model of size distributions among species of animals. Am. Nat. 93: 117-125.

Inniss L., Simcock A., Ajawin A.Y., Alcala A. C., Bernal P., Calumpong H., P., Araghi P. E., Green S.O., Harris P., Kamara O.K., Kohata K., Marschoff E., Martin G., Ferreira B.P., Park C., Payet R.A., Rice J., Rosenberg A., Ruwa R., Tuhumwire J.T., Van Gaever S., Wang J., Wesławski J.M. 2016. The First Global Integrated Marine Assessment World Ocean AssessmentI.

James F.C. 1970. Geographic size variation in birds and its relationship to climate. Ecology. 51:365-390.

Jarvis E., Mirarab S., Aberer A., Li B., Houde P., Li C., Ho S.Y.W, Faircloth B., Nabholz B . , Howard J., Suh A. 2014. Whole-genome analyses resolve early branches in the tree of life of modern birds. Science (80-. ). 346:1320–31.

Jombart T., Balloux F., Dray S. 2010. Adephylo: new tools for investigating the phylogenetic signal in biological traits. Bioinformatics. 26:1907–1909.

Karin B.R., Gamble T. Jackman T.R. 2019. Optimizing phylogenomics with rapidly evolving long exons: comparison with anchored hybrid enrichment and ultraconserved elements. *bioRxiv*, 672238.

Kass R., Raftery A. 1995. Bayes factors. J. Am. Stat. Assoc. 90:773–795.

Katoh K., Kuma K.I., Toh H., Miyata T. 2005. MAFFT version 5: Improvement in accuracy of multiple sequence alignment. Nucleic Acids Res. 33:511–518.

Kennedy M., Page R.D.M., Prum R. 2002. Seabird supertrees: combining partial estimates of procellariiform phylogeny. Auk. 119:88–108.

Kelt D.A., and Meyer M. D. 2009. Body size frequency distributions in African mammals are bimodal at all spatial scales. Glob. Ecol. Biogeogr. 18:19-29.

Kimura M. 1979. The Neutral Theory of Molecular Evolution. 241:98–129.

Lanfear R., Frandsen P.B., Wright A.M., Senfeld T., Calcott B. 2017. Partitionfinder 2: New methods for selecting partitioned models of evolution for molecular and morphological phylogenetic analyses. Mol. Biol. Evol. 34:772–773.

Lanfear R., Ho S.Y.W., Jonathan Davies T., Moles A.T., Aarssen L., Swenson N.G., Warman L., Zanne A.E., Allen A.P. 2013. Taller plants have lower rates of molecular evolution. Nat. Commun. 4:1–7.

Lanfear R., Ho S.Y.W., Love D., Bromham L. 2010. Mutation rate is linked to diversification in birds. Proc. Natl. Acad. Sci. 107:20423–20428.

Leaché A.D., Fujita M.K., Minin V.N., Bouckaert R.R. 2014. Species delimitation using genome-wide SNP Data. Syst. Biol. 63:534–542.

Li W.H. 1993. Unbiased estimation of the rates of synonymous and nonsynonymous substitution. J. Mol. Evol. 36:96–99.

Lockley, R.M. 1967. Animal Navigation. Pan Books. pp. 114–117.

Longo S.J., Faircloth B.C., Meyer A., Westneat M.W., Alfaro M.E., Wainwright P.C. 2017. Phylogenomic analysis of a rapid radiation of misfit fishes (Syngnathiformes) using ultraconserved elements. Mol. Phylogenet. Evol. 113:33–48.

Loughrey, C. 2018. 'Blue Planet' most watched show of 2017 as top 10 announced. The Independent.

Manthey J.D., Campillo L.C., Burns K.J., Moyle R.G. 2016. Comparison of target-capture and restriction-site associated DNA sequencing for phylogenomics: A test in cardinalid tanagers (Aves, Genus: Piranga). Syst. Biol.65:640–650.

Martin A.P., Palumbi S.R. 1993. Body size, metabolic rate, generation time, and the molecular clock. Proc. Natl. Acad. Sci. 90:4087–4091.

Mayr G., Smith T. 2012. Phylogenetic affinities and taxonomy of the Oligocene Diomedeoididae, and the basal divergences amongst extant procellariiform birds. Zool. J. Linn. Soc. 166:854–875.

McCormack J.E., Faircloth B.C., Crawford N.G., Gowaty P.A., Brumfield R.T., Glenn T.C. 2012. Ultraconserved elements are novel phylogenomic markers that resolve placental mammal phylogeny when combined with species-tree analysis. Genome Res., 22(4), 746-754.

Mccormack J.E., Faircloth B.C., Crawford N.G., Gowaty P.A., Brumfield R.T., Glenn T.C. 2012. Ultraconserved elements are novel phylogenomic markers that resolve placental mammal phylogeny when combined with species tree analysis. Genome Res. 22:746–754.

McCormack J.E., Harvey M.G., Faircloth B.C., Crawford N.G., Glenn T.C., Brumfield R.T. 2013. A Phylogeny of Birds Based on Over 1,500 Loci collected by target enrichment and high-throughput sequencing. PLoS One. 8.

Meiri S., Dayan T. 2003. On the validity of Bergmann's rule. J Biogeogr. 30:331-351.

Menkhorst P.W. 1984. Use of nest boxes by forest vertebrates in gippsland: Acceptance, preference and demand. Wildl. Res. 11:255–264.

Metropolis N., Rosenbluth A.W., Rosenbluth M.N., Teller A.H., Teller E. 1953. Equations of state calculations by fast computing machines. J. Chem. Phys. 21:1087-1092.

Mooers A., Harvey P.H. 1994. Metabolic rate, generation time, and the rate of molecular evolution in birds. Mol. Phylogenet. Evol. 3:344–350.

Nabholz B., Glémin S., Galtier N. 2009. The erratic mitochondrial clock: Variations of mutation rate, not population size, affect mtDNA diversity across birds and mammals. BMC Evol. Biol. 9:1–13.

Nabholz B., Uwimana N., Lartillot N. 2013. Reconstructing the phylogenetic history of long- term effective population size and life-history traits using patterns of amino acid replacement in mitochondrial genomes of mammals and birds. Genome Biol. Evol. 5:1273–1290.

Nagy K.A. 2005. Field metabolic rate and body size. J. Exp. Biol. 208:1621–1625.

Nascimento F.F., dos Reis M., Yang Z. 2017. A biologist's guide to Bayesian phylogenetic analysis. Nat. Ecol. Evol. 1:1446.

Nguyen L.T., Schmidt H.A., Von Haeseler A., Minh B.Q. 2015. IQ-TREE: A fast and effective stochastic algorithm for estimating maximum-likelihood phylogenies. Mol. Biol. Evol. 32:268–274.

Nunn G., Stanley S. 1998. Body size effects and rates of cytochrome b evolution in tube-nosed seabirds. Mol. Biol. Evol. 15:1360–1371.

Ohta T. 1972. Population size and rate of evolution. J. Mol. Evol. 1:305–314.

Ohta T. 1973. Slightly deleterious mutant substitutions in evolution. Nature. 246:96–97.

Olson V.A., Davies R.G., Orme C.D.L., Thomas G.H., Meiri S., Blackburn T.M., Gaston K.J., Owens I.P.F, Bennett P.M. 2009. Global biogeography and ecology of body size in birds. Ecol. Lett. 12:249-259.

Orme D. 2013. The caper package: comparative analysis of phylogenetics and evolution in R. R Packag. version 5.2. 5:1–36.

Paradis E., Schliep K. 2018. ape 5.0: an environment for modern phylogenetics and evolutionary analyses in R. Bioinformatics.

Patané J.S.L., Weckstein J.D., Aleixo A., Bates J.M. 2009. Evolutionary history of Ramphastos toucans: Molecular phylogenetics, temporal diversification, and biogeography. Mol. Phylogenet. Evol. 53:923–934.

Penhallurick J., Wink M. 2004. Analysis of the taxonomy and nomenclature of the Procellariiformes based on complete nucleotide sequences of the mitochondrial cytochrome b gene. Emu. 104:125–147.

Pereira S.L., Baker A.J. 2006. A mitogenomic timescale for birds detects variable phylogenetic rates of molecular evolution and refutes the standard molecular clock. Mol. Biol. Evol. 23:1731–1740.

Philippe H., Brinkmann H., Lavrov D. V., Littlewood D.T.J., Manuel M., Wörheide G., Baurain D. 2011. Resolving difficult phylogenetic questions: why more sequences are not enough. PLoS Biol. 9:e1000602.

Pickering, S.P.C., Berrow, S.D. 2001. Courtship behaviour of the Wandering Albatross Diomedea exulans at Bird Island, South Georgia. Mar. Ornithol. 29:29–37.

Pinheiro J., Bates D., DebRoy A., Sarkar D., R Core Team. 2018. nlme: Linear and Nonlinear Mixed Effects Models. R Packag. version 3.1-137.

Prum R.O., Berv J.S., Dornburg A., Field D.J., Townsend J.P., Lemmon E.M., Lemmon A.R. 2015. A comprehensive phylogeny of birds (Aves) using targeted next-generation DNA sequencing. Nature. 526:569–573.

R Core Team. 2018. R: a language and environment for statistical computing. Vienna, Austria: R Foundation for Statistical Computing.

Rambaut A. 2017. FigTree-version 1.4. 3, a graphical viewer of phylogenetic trees.

Rambaut A., Drummond A.J., Xie D., Baele G., Suchard M.A. 2018. Posterior Summarization in Bayesian Phylogenetics Using Tracer 1.7. Syst. Biol.67:901–904.

Reddy S., Kimball R.T., Pandey A., Hosner P.A., Braun M.J., Hackett S.J., Han K.L., Harshman J., Huddleston C.J., Kingston S., Marks B.D., Miglia K.J., Moore W.S., Sheldon F.H., Witt C.C., Yuri T., Braun E.L. 2017. Why do phylogenomic data sets yield conflicting trees? Data type influences the avian tree of life more than taxon sampling. Syst. Biol. 66:857–879.

Rodriguez F.J., Oliver J.L., Marin A., Medina, J.R. 1990. The general stochastic model of nucleotide substitution. Journal of theoretical biology. 142:485-501.

Rodríguez A., Arcos J. M., Bretagnolle V., Dias M. P., Holmes N. D., Louzao M., Provencher J., Raine A.F., Ramirez N.D., Rodriguez B., Ronconi, R. A., Taylor R.S., Bonnaud E., Borrelle S.B., Cortes V., Descamps S., Friesen V.L., Genovart M., Hedd A., Hodum P., Humphries G.R.W, Le Corre M., Lebarbenchon C., Martin R., Melvin E.F., Montevecchi W.A., Pinet P., Pollet I.L., Ramos R., Russell J.C., Ryan P.G., Sanz-Aguilar A., Spatz D.R., Travers M., Votier S.C., Wanless R.M., Woehler E., Chiaradia A. (2019). Future directions in conservation researchon petrels and shearwaters. Front Mar Sci, 6:94.

Rokas A., Carroll S.B. 2006. Bushes in the Tree of Life. PLoS Biol. 4:e352.

Roman L., Hardesty B.D., Hindell M.A., Wilcox C. 2019. A quantitative analysis linking seabird mortality and marine debris ingestion. Sci. Rep., 9:3202.

Rosenzweig M.L. 1968. The strategy of body size in mammalian carnivores. Am. Midl. Nat. 1:299-315.

Shaffer, S.A., Tremblay, Y., Weimerskirch, H., Scott, D., Thompson, D.R., Sagar, P.M., Moller, H., Taylor, G.A., Foley, D.G., Block, B.A., D.P., Costa. 2006. Migratory shearwaters integrate oceanic resources across the Pacific Ocean in an endless summer. Proc. Natl. Acad. Sci. 103 (34): 12799–12802.

Saastamoinen M., Bocedi G., Cote J., Legrand D., Guillaume F., Wheat C.W., Fronhofer E.A., Garcia C., Henry R., Husby A., Baguette M., Bonte D., Coulon A., Kokko H., Matthysen E., Niitepold K., Nonaka E., Stevens V., Travis J., Donohue K., Bullock J., Delgado M.M. 2018. Genetics of dispersal. Biol. Rev. 93:574-599.

Sandelin A., Bailey P., Bruce S., Engström P.G., Klos J.M., Wasserman W.W., Ericson J., Lenhard B. 2004. Arrays of ultraconserved non-coding regions span the loci of key developmental genes in vertebrate genomes. BMC Genomics. 5:1–9.

Sayyari E., Mirarab S. 2016. Fast coalescent-based computation of local branch support from quartet frequencies. Mol. Biol. Evol. 33:1654–1668.
Schreiber E., Burger J. 2002. Biology of marine birds. Boca Raton, FL: CRC Press.
Sibley C. G., Ahlquist J. E. 1990. Phylogeny and classification of birds: a study in molecular evolution. Yale University Press.
Simmons G.F. 1927. Sinbads of Science: Narrative of a Windjammer's Specimen-Collecting Voyage to the Sargasso Sea, to Senegambian Africa and among Islands of High Adventure in the South Atlantic. National Geographic Magazine. 52:1-75.
Smith S.A., Beaulieu J.M. 2009. Life history influences rates of climatic niche evolution in flowering plants. Proc. R. Soc. B Biol. Sci. 276:4345–4352.
Stamatakis A. 2014. RAxML version 8: A tool for phylogenetic analysis and post-analysis of large phylogenies. Bioinformatics. 30:1312–1313.
Steiper M.E., Seiffert E.R. 2012. Evidence for a convergent slowdown in primate molecular rates and its implications for the timing of early primate evolution. Proc. Natl. Acad. Sci. 109:6006–6011.
Suh A., Smeds L., Ellegren H. 2015. The dynamics of incomplete lineage sorting across the ancient adaptive radiation of neoavian birds. PLoS Biol. 13:1–18.
Sukumaran J., Holder M.T. 2010. DendroPy: A Python library for phylogenetic computing. Bioinformatics. 26:1569–1571.
Sydeman W.J., Thompson S.A., Kitaysky A. 2012. Seabirds and climate change: Roadmap for the future. Mar. Ecol. Prog. Ser. 454:107–117.
Tagliacollo V.A., Lanfear R. 2018. Estimating improved partitioning schemes for ultraconserved elements. Mol. Biol. Evol. 35:1798–1811.
Tamura K., Battistuzzi F.U., Billing-Ross P., Murillo O., Filipski A., Kumar S. 2012. Estimating divergence times in large molecular phylogenies. Proc. Natl. Acad. Sci. 109:19333–19338.
Thomas J.A., Welch J.J., Lanfear R., Bromham L. 2010. A generation time effect on the rate of molecular evolution in invertebrates. Mol. Biol. Evol. 27:1173–1180.
Thomas J.A., Welch J.J., Woolfit M., Bromham L. 2006. There is no universal molecular clock for invertebrates, but rate variation does not scale with body size. Proc. Natl. Acad. Sci. 103:7366–7371.
Taylor R.S. 2017. Parallel divergence by allochrony and cryptic speciation in two highly pelagic seabird species complexes (*Hydrobates*spp.). Queen's University, Kingston, Ontario, Canada.
Taylor R.S., Bolton M., Beard A., Birt T., Deane-Coe P., Raine A. F., Gonzalez-Solis J., Lougheed S.C. & Friesen V. L. 2019. Cryptic species and independent origins of allochronic populations within a seabird species complex (Hydrobates spp.). Mol Phylogenet Evol. 139:106552.
Tong K.J, Duchene D.A., Duchene S., Geoghegan J.L, Ho, S.Y.W. 2018. A comparison of methods for estimating substitution rates from ancient DNA sequence data. BMC Evol. Biol. 18:70.
Wang X., Clarke J.A. 2014. Phylogeny and forelimb disparity in waterbirds. Evolution.

68:2847–2860.
Warham J. 1990. The Petrels: Their ecology and breeding systems. Academic Press.
Weber C.C., Nabholz B., Romiguier J., Ellegren H. 2014. K r/K c but not dN/dS correlates positively with body mass in birds , raising implications for inferring lineage-specific selection. Genome Biol. 15:542.
Weir J.T., Schluter D. 2008. Calibrating the avian molecular clock. Mol. Ecol. 17:2321–2328.
Welch J.J., Bininda-Emonds O.R.P., Bromham L. 2008. Correlates of substitution rate variation in mammalian protein-coding sequences. BMC Evol. Biol. 8:1–12.
Whitfield J.B., Lockhart P.J. 2007. Deciphering ancient rapid radiations. Trends Ecol. Evol. 22:258–265.
Wickham H. 2016. ggplot2: Elegant Graphics for Data Analysis. New York: Springer-Verlag.
Wiens J.J., Kuczynski C.A., Smith S.A., Mulcahy D.G., Sites J.W., Townsend T.M., Reeder T.W. 2008. Branch lengths, support, and congruence: Testing the phylogenomic approach with 20 nuclear loci in snakes. Syst. Biol. 57:420–431.
Wilcox C., Van Sebille E., Denise Hardesty B. 2015. Threat of plastic pollution to seabirds is global, pervasive, and increasing. Proc Natl Acad Sci. 112:11899–11904
Woolfe A., Goodson M., Goode D.K., Snell P., McEwen G.K., Vavouri T., Smith S.F., North P., Callaway H., Kelly K., Walter K., Abnizova I., Gilks W., Edwards Y.J.K., Cooke J.E., Elgar G. 2005. Highly conserved non-coding sequences are associated with vertebrate development. PLoS Biol. 3.
Woolfit M., Bromham L. 2003. Increased rates of sequence evolution in endosymbiotic bacteria and fungi with small effective population sizes. Mol. Biol. Evol. 20:1545–1555.
Woolrich M.W., Jbabdi S., Patenaude B., Chappell M., Makni S., Behrens T., Beckmann C., Jenkinson M., Smith, S.M. 2009. Bayesian analysis of neuroimaging data in FSL. Neuroimage 45:173-S186.
Zhang C., Rabiee M., Sayyari E., Mirarab S. 2018. ASTRAL-III: polynomial time species tree reconstruction from partially resolved gene trees. BMC bioinformatics. 19:153.
Zeveloff S.I. Boyce M.S. 1988. Body size patterns in North American mammalian faunas. Evolution of life histories of mammals. Yale University Press, New Haven, Connecticut, USA.

# SUPPLEMENTARY MATERIAL

| Species | Sampling location | Accession number | Sample from |
|---|---|---|---|
| *Aphrodroma brevirostris* | Gough Island | KGP-1 | Gary Nunn |
| *Bulweria bulwerii* | Madeira | E006980 | Vincent Bretagnolle |
| *Calonectris diomedea* | Off Cape Hatteras National Seashore, NC, USA | USNM_620710 | Smithsonian Institution |
| *Calonectrisleucomelas* | Mikura Islands, Japan | Cleu15 | Jacob Gonzalez-Solis |
| *Daption capense* | Muriwai Beach, North Island, New Zealand | KU_21827 | The University of Kansas Natural History Museum |
| *Diomedea dabbenena* | Gough Island | Nunn_WA-3 | Gary Nunn |
| *Fregetta grallarialeucogaster* | Gough Island | Nunn_WBSP2 | Gary Nunn |
| *Fulmarus glacialisauduboni* | North of Keflavik, Iceland | USNM_623297 | Smithsonian Institution |
| *Garrodia nereis* | Gough Island | Nunn_GBSP3 | Gary Nunn |
| *Halobaena caerulea* | South Georgia | UWBM_61675 | Burke Museum, University of Washington |
| *Hydrobates pelagicus* | Malta | Bretagnolle_MSP1 | Vincent Bretagnolle |
| *Macronectes giganteus* | Gough Island | Nunn_SPG-G-1 | Gary Nunn |
| *Nesofregetta fuliginosa* | South Pacific | USNM_614206 | Smithsonian Institution |
| *Oceanites oceanicusoceanicus* | San Antonio, Region de Valparaiso, Chile | AMNH_DOT3175 | American Museum of Natural History |
| *Oceanodroma castro* | Nelson, Virginia, USA | USNM_602013 | Smithsonian Institution |
| *Oceanodroma furcata furcata* | Alaska, USA | USNM_638711 | Smithsonian Institution |
| *Oceanodroma leucorhoa* | Unalga Pass, East of Dutch Harbor, Alaska, USA | USNM_639040 | Smithsonian Institution |
| *Oceanodroma tethys tethys* | Galapagos Islands, Ecuador | LSU_B15454 | Louisiana State University |
| *Pachyptila desolata* | Towradgi, New South Wales, Australia | UWBM_76646 | Burke Museum, University of Washington |
| *Pachyptila turtur* | Southwest of Cape Foulwind, New Zealand | UWBM_81011 | Burke Museum, University of Washington |

| | | | |
|---|---|---|---|
| *Pagodroma nivea* | South Georgia | UWBM_61674 | Burke Museum, University of Washington |
| *Pelagodroma marina maoriana* | North Pacific Ocean | USNM_614205 | Smithsonian Institution |
| *Pelecanoides magellani* | Puerto Williams, Navarino Island, Chile | AMNH_DOT3211 | American Museum of Natural History |
| *Pelecanoides urinatrix exsul* | Annenkov Island, South Georgia | UWBM_60517 | Burke Museum, University of Washington |
| *Phoebastria albatrus* | Aleutian Islands, Alaska, USA | UWBM_55909 | Burke Museum, University of Washington |
| *Phoebastriaimmutabilis* | Hawaii, USA | USNM_643358 | Smithsonian Institution |
| *Phoebetria fusca* | Gough Island | Nunn_SA-3 | Gary Nunn |
| *Procellaria cinerea* | Gough Island | Nunn_GYP-2 | Gary Nunn |
| *Procellariawestlandica* | East Cape, New Zealand | UWBM_82803 | Burke Museum, University of Washington |
| *Pseudobulweria becki* | At sea | Bretagnolle_beckiS1 | Vincent Bretagnolle |
| *Pseudobulweria macgillivrayi* | Fiji | KU_22549 | The University of Kansas Natural History Museum |
| *Pseudobulweriarostrata rostrata* | American Samoa | NZP_7491 | Smithsonian's National Zoo |
| *Pterodroma cookii* | Grayland, Washington, USA | UWBM_70582 | Burke Museum, University of Washington |
| *Pterodroma hasitata hasitata* | St Michaels, Miles River, Maryland, USA | USNM_621363 | Smithsonian Institution |
| *Pterodroma hypoleuca* | North Pacific Ocean | UWBM_55680 | Burke Museum, University of Washington |
| *Pterodroma incerta* | Gough Island | Nunn_ATP-3 | Gary Nunn |
| *Pterodroma neglecta neglecta* | Pitcairn Islands | USNM_562779 | Smithsonian Institution |
| *Pterodromanigripennis* | New Caledonia | Bretagnolle_PEAN12 | Vincent Bretagnolle |
| *Pterodromasandwichensis* | Maui | NZP_HAPE 21298 | Smithsonian's National Zoo |
| *Pterodroma ultima* | Pitcairn Islands | USNM_562778 | Smithsonian Institution |
| *Puffinus assimilis elegans* | Amsterdam Island | MNHN1990-796 | Vincent Bretagnolle |
| *Puffinus carneipes* | Ocean off Albany, Western Australia | AMNH_DOT17805 | American Museum of Natural History |
| *Puffinus griseus* | Kidney island, Falklands | Agri2 | Jacob Gonzalez-Solis |
| *Puffinus huttoni* | New Zealand | LSU_B23388 | Louisiana State University |

| | | | |
|---|---|---|---|
| *Puffinus lherminieri baroli* | Tenerife, Canary Islands | PAAs91 | Austin |
| *Puffinus nativitatis* | North Pacific Ocean | USNM_613922 | Smithsonian Institution |
| *Puffinus newelli* | NA | NESH_10250 | Smithsonian's National Zoo |
| *Puffinus pacificus* | Sand Island, Johnston Atoll | Apac76 | Austin |
| *Thalassarche cautasalvini* | Bounty Platform, New Zealand | UWBM_81006 | Burke Museum, University of Washington |
| *Thalassarche chrysostoma* | Diego Ramirez, Chile | AMNH_DOT2584 | American Museum of Natural History |
| *Ciconia maguari (outgroup)* | Estancia El Tala, Near Puerto Constanza, Entre Rios, Argentina | USNM_614527 | Smithsonian Institution |
| *Spheniscus demersus(outgroup)* | Captive | USNM_631252 | Smithsonian Institution |
| *Sula leucogaster(outgroup)* | Johnston Atoll | USNM_622596 | Smithsonian Institution |

Table S1. Information about samples included in this study

| Species | A | T | G | C | G+C |
|---|---|---|---|---|---|
| *Aphrodroma brevirostris* | 0,3046 | 0,3047 | 0,1954 | 0,1953 | 0,3907 |
| *Bulweria bulwerii* | 0,3041 | 0,3047 | 0,1955 | 0,1957 | 0,3912 |
| *Calonectris diomedea* | 0,3043 | 0,3048 | 0,1953 | 0,1956 | 0,3909 |
| *Calonectris leucomelas* | 0,3042 | 0,3048 | 0,1954 | 0,1955 | 0,3910 |
| *Cicoinia maguari* | 0,3039 | 0,3047 | 0,1957 | 0,1958 | 0,3914 |
| *Daption capense* | 0,3041 | 0,3046 | 0,1958 | 0,1955 | 0,3913 |
| *Diomedea dabbenena* | 0,3042 | 0,3048 | 0,1954 | 0,1956 | 0,3910 |
| *Fregetta grallaria leucogaster* | 0,3042 | 0,3048 | 0,1954 | 0,1956 | 0,3910 |
| *Fulmarus glacialis auduboni* | 0,3039 | 0,3046 | 0,1957 | 0,1957 | 0,3915 |
| *Garrodia nereis* | 0,3047 | 0,3050 | 0,1951 | 0,1952 | 0,3904 |
| *Halobaena caerulea* | 0,3039 | 0,3046 | 0,1958 | 0,1957 | 0,3915 |
| *Hydrobates pelagicus* | 0,3042 | 0,3047 | 0,1953 | 0,1958 | 0,3911 |
| *Macronectes giganteus* | 0,3042 | 0,3047 | 0,1954 | 0,1956 | 0,3910 |
| *Nesofregetta fuliginosa* | 0,3040 | 0,3048 | 0,1955 | 0,1956 | 0,3911 |
| *Oceanites oceanicus oceanicus* | 0,3044 | 0,3051 | 0,1953 | 0,1953 | 0,3906 |
| *Oceanodroma castro* | 0,3039 | 0,3046 | 0,1958 | 0,1957 | 0,3915 |
| *Oceanodroma furcata furcata* | 0,3044 | 0,3049 | 0,1952 | 0,1956 | 0,3907 |
| *Oceanodroma leucorhoa* | 0,3041 | 0,3041 | 0,1959 | 0,1960 | 0,3918 |
| *Oceanodroma tethys tethys* | 0,3041 | 0,3046 | 0,1956 | 0,1957 | 0,3912 |
| *Pachyptila desolata* | 0,2963 | 0,2984 | 0,2023 | 0,2031 | 0,4054 |
| *Pachyptila turtur* | 0,3043 | 0,3045 | 0,1956 | 0,1956 | 0,3911 |
| *Pagodroma nivea* | 0,3042 | 0,3045 | 0,1956 | 0,1957 | 0,3913 |
| *Pelagodroma marina maoriana* | 0,3045 | 0,3051 | 0,1952 | 0,1952 | 0,3904 |
| *Pelecanoides magellani* | 0,3043 | 0,3052 | 0,1952 | 0,1954 | 0,3905 |
| *Pelecanoides urinatrix exsul* | 0,3047 | 0,3052 | 0,1951 | 0,1950 | 0,3901 |
| *Phoebastria albatrus* | 0,3040 | 0,3048 | 0,1955 | 0,1957 | 0,3912 |
| *Phoebastria immutabilis* | 0,3045 | 0,3050 | 0,1952 | 0,1953 | 0,3905 |
| *Phoebetria fusca* | 0,3042 | 0,3048 | 0,1953 | 0,1957 | 0,3910 |
| *Procellaria cinerea* | 0,3044 | 0,3047 | 0,1954 | 0,1955 | 0,3909 |
| *Procellaria westlandica* | 0,3030 | 0,3042 | 0,1963 | 0,1965 | 0,3928 |
| *Pseudobulweria becki* | 0,3044 | 0,3049 | 0,1954 | 0,1953 | 0,3906 |
| *Pseudobulweria macgillivrayi* | 0,3037 | 0,3043 | 0,1959 | 0,1961 | 0,3920 |
| *Pseudobulweria rostrata rostrata* | 0,3043 | 0,3049 | 0,1953 | 0,1954 | 0,3907 |
| *Pterodroma cookii* | 0,3044 | 0,3048 | 0,1953 | 0,1955 | 0,3908 |
| *Pterodroma hasitata hasitata* | 0,3042 | 0,3046 | 0,1954 | 0,1958 | 0,3912 |
| *Pterodroma hypoleuca* | 0,3006 | 0,3013 | 0,1991 | 0,1991 | 0,3982 |
| *Pterodroma incerta* | 0,3037 | 0,3039 | 0,1958 | 0,1965 | 0,3924 |

| | | | | | |
|---|---|---|---|---|---|
| *Pterodroma neglecta neglecta* | 0,3042 | 0,3045 | 0,1955 | 0,1958 | 0,3913 |
| *Pterodroma nigripennis* | 0,3040 | 0,3046 | 0,1958 | 0,1956 | 0,3915 |
| *Pterodroma sandwichensis* | 0,3043 | 0,3046 | 0,1955 | 0,1955 | 0,3911 |
| *Pterodroma ultima* | 0,3041 | 0,3048 | 0,1953 | 0,1958 | 0,3911 |
| *Puffinus assimilis elegans* | 0,3037 | 0,3037 | 0,1963 | 0,1963 | 0,3926 |
| *Puffinus carneipes* | 0,3038 | 0,3043 | 0,1959 | 0,1960 | 0,3918 |
| *Puffinus griseus* | 0,3041 | 0,3044 | 0,1959 | 0,1956 | 0,3915 |
| *Puffinus huttoni* | 0,3041 | 0,3045 | 0,1957 | 0,1957 | 0,3914 |
| *Puffinus lherminieri baroli* | 0,3039 | 0,3046 | 0,1957 | 0,1959 | 0,3916 |
| *Puffinus nativitatis* | 0,3037 | 0,3043 | 0,1960 | 0,1960 | 0,3920 |
| *Puffinus newelli* | 0,3042 | 0,3042 | 0,1958 | 0,1957 | 0,3915 |
| *Puffinus pacificus* | 0,3036 | 0,3043 | 0,1960 | 0,1961 | 0,3921 |
| *Spheniscus demersus* | 0,3042 | 0,3047 | 0,1954 | 0,1957 | 0,3911 |
| *Sula leucogaster* | 0,3030 | 0,3044 | 0,1963 | 0,1963 | 0,3926 |
| *Thalassarche cauta salvini* | 0,3043 | 0,3046 | 0,1956 | 0,1955 | 0,3911 |
| *Thalassarche chrysostoma* | 0,3042 | 0,3046 | 0,1955 | 0,1956 | 0,3912 |

Table S2. GC content for each species.

| Species | Body mass (g) | Source |
|---|---|---|
| Aphrodroma_brevirostris_Nunn_KGP_1 | 357,5 | Schramm 1983* |
| Bulweria_bulwerii_Bretagnolle_E006980 | 103,5 | Brooke 2004** |
| Calonectris_diomedea_USNM_620710 | 839,5 | Brooke 2004 |
| Calonectris_leucomelas_Spanish_Cleu13 | 507,0 | Brooke 2004 |
| Daption_capense_KU_21827 | 463,5 | Brooke 2004 |
| Diomedea_dabbenena_Nunn_WA3 | 7050,0 | Handbook of the Birds*** |
| Fregetta_grallaria_leucogaster_Nunn_WBSP2 | 54,0 | Brooke 2004 |
| Fulmarus_glacialis_auduboni_USNM_623297 | 767,5 | Brooke 2004 |
| Garrodia_nereis_Nunn_GBSP3 | 34,0 | Brooke 2004 |
| Halobaena_caerulea_UWBM_61675 | 196,5 | Brooke 2004 |
| Hydrobates_pelagicus_Bretagnolle_MSP1 | 27,6 | Scott 1970**** |
| Macronectes_giganteus_Nunn_SPGG1 | 4440,0 | Brooke 2004 |
| Nesofregetta_fuliginosa_USNM_614206 | 67,0 | Handbook of the Birds of the World |
| Oceanites_oceanicus_oceanicus_AMNH_DOT3175 | 34,7 | Handbook of the Birds of the World |
| Oceanodroma_castro_USNM_602013 | 46,7 | Brooke 2004 |
| Oceanodroma_furcata_furcata_USNM_638711 | 58,8 | Brooke 2004 |
| Oceanodroma_leucorhoa_USNM_639040 | 45,3 | Brooke 2004 |
| Oceanodroma_tethys_tethys_LSU_B15454 | 25,5 | Brooke 2004 |
| Pachyptila_desolata_UWBM_76646 | 156,5 | Brooke 2004 |
| Pachyptila_turtur_UWBM_81011 | 139,1 | Brooke 2004 |
| Pagodroma_nivea_UWBM_61674 | 290,8 | Brooke 2004 |
| Pelagodroma_marina_maoriana_USNM_614205 | 50,4 | Brooke 2004 |
| Pelecanoides_magellani_AMNH_DOT3211 | 162,0 | Brooke 2004 |
| Pelecanoides_urinatrix_exsul_UWBM_60517 | 153,9 | Brooke 2004 |
| Phoebastria_albatrus_UWBM_55909 | 6300,0 | Brooke 2004 |
| Phoebastria_immutabilis_USNM_643358 | 2350,0 | Brooke 2004 |
| Phoebetria_fusca_Nunn_SA3 | 2485,0 | Handbook of the Birds of the World |
| Procellaria_cinerea_Nunn_GYP2 | 1031,0 | Brooke 2004 |
| Procellaria_westlandica_UWBM_82803 | 999,5 | Brooke 2004 |
| Pseudobulweria_becki_Bretagnolle_beckiS1 | 150,0 | Handbook of the Birds of the World |
| Pseudobulweria_macgillivrayi_KU_22549 | 131,5 | Handbook of the Birds of the World |
| Pseudobulweria_rostrata_rostrata_NZP | 355,0 | Brooke 2004 |
| Pterodroma_cookii_UWBM_70582 | 178,5 | Brooke 2004 |

| | | |
|---|---|---|
| Pterodroma_hasitata_hasitata_USNM_621363 | 460,5 | Handbook of the Birds of the World |
| Pterodroma_hypoleuca_UWBM_55680 | 176,5 | Brooke 2004 |
| Pterodroma_incerta_Nunn_ATP3 | 522,5 | Handbook of the Birds of the World |
| Pterodroma_neglecta_neglecta_USNM_562779 | 439,5 | Brooke 2004 |
| Pterodroma_nigripennis_Bretagnolle_PEAN12 | 174,1 | Brooke 2004 |
| Pterodroma_sandwichensis_NZP_HAPE_21298 | 434,3 | Brooke 2004 |
| Pterodroma_ultima_USNM_562778 | 435,0 | Brooke 2004 |
| Puffinus_assimilis_elegans_Bretagnolle_MNHN1990_796 | 155,8 | Brooke 2004 |
| Puffinus_carneipes_AMNH_DOT17805 | 612,2 | Brooke 2004 |
| Puffinus_griseus_Spanish_Agri2 | 434,0 | Brooke 2004 |
| Puffinus_huttoni_LSU_B23388 | 303,0 | Handbook of the Birds of the World |
| Puffinus_lherminieri_baroli_Spanish_PAASs91 | 193,0 | Brooke 2004 |
| Puffinus_nativitatis_USNM_613922 | 337,5 | Brooke 2004 |
| Puffinus_newelli_NZP_NESH_10250 | 342,8 | Handbook of the Birds of the World |
| Puffinus_pacificus_Spanish_Apac76 | 389,3 | Brooke 2004 |
| Thalassarche_cauta_salvini_UWBM_81006 | 4025,0 | Brooke 2004 |
| Thalassarche_chrysostoma_AMNH_DOT2584 | 3645,0 | Brooke 2004 |
| Thalassoica_antarctica_UWBM_81012 | 735,0 | Brooke 2004 |

Table S3. Body mass data included in the PGLS models and sources.

| Species | Age (years) | Source |
|---|---|---|
| Bulweria_bulwerii_Bretagnolle_E006980 | 6 | [1] and [2] |
| Calonectris_diomedea_USNM_620710 | 9 | [1] and [3] |
| Calonectris_leucomelas_Spanish_Cleu13 | 9 | [1] |
| Daption_capense_KU_21827 | 5,5 | [1] and [4] |
| Diomedea_dabbenena_Nunn_WA3 | 10 | [5] |
| Fregetta_grallaria_leucogaster_Nunn_WBSP2 | 4,5 | [6] |
| Fulmarus_glacialis_auduboni_USNM_623297 | 9 | [1] and [7] |
| Garrodia_nereis_Nunn_GBSP3 | 5 | [8] |
| Halobaena_caerulea_UWBM_61675 | 4 | [9] |
| Hydrobates_pelagicus_Bretagnolle_MSP1 | 4,5 | [10] |
| Macronectes_giganteus_Nunn_SPGG1 | 7,5 | [1] |
| Oceanites_oceanicus_oceanicus_AMNH_DOT3175 | 3 | [11] |
| Oceanodroma_castro_USNM_602013 | 3 | [12] |
| Oceanodroma_leucorhoa_USNM_639040 | 5 | [1] |
| Pachyptila_desolata_UWBM_76646 | 5 | [1] |
| Pachyptila_turtur_UWBM_81011 | 4,5 | [14] |
| Pagodroma_nivea_UWBM_61674 | 9,9 | [1] |
| Pelagodroma_marina_maoriana_USNM_614205 | 3 | [11] |
| Pelecanoides_magellani_AMNH_DOT3211 | 2 | [1] |
| Pelecanoides_urinatrix_exsul_UWBM_60517 | 2 | [1] |
| Phoebastria_albatrus_UWBM_55909 | 9 | [1] |
| Phoebastria_immutabilis_USNM_643358 | 9 | [1] and [2] |
| Phoebetria_fusca_Nunn_SA3 | 12,7 | [1] |
| Procellaria_cinerea_Nunn_GYP2 | 10 | [1] |
| Procellaria_westlandica_UWBM_82803 | 10 | [1] |
| Pterodroma_hasitata_hasitata_USNM_621363 | 7 | [13] |
| Pterodroma_sandwichensis_NZP_HAPE_21298 | 5,5 | [2] |
| Puffinus_carneipes_AMNH_DOT17805 | 6 | [1] |
| Puffinus_griseus_Spanish_Agri2 | 6 | [1] and [15] |
| Puffinus_huttoni_LSU_B23388 | 5 | [16] |
| Puffinus_lherminieri_baroli_Spanish_PAASs91 | 8 | [1] |
| Puffinus_nativitatis_USNM_613922 | 4 | [2] |
| Puffinus_newelli_NZP_NESH_10250 | 6 | [2] |
| Puffinus_pacificus_Spanish_Apac76 | 6 | [2] |
| Thalassarche_cauta_salvini_UWBM_81006 | 12 | [17] |
| Thalassarche_chrysostoma_AMNH_DOT2584 | 13 | [1] and [18] |
| Puffinus_assimilis | 5 | [19] |

[1] Brooke, M. de L. 2004. Albatrosses and petrels across the World. Oxford University Press, Oxford.
[2] Hawaii's Comprehensive Wildlife Conservation Strategy October 1, 2005.
[3] Mougin, J. L., Jouanin, C., Roux, F., & Zino, F. (2000). Fledging weight and juvenile survival of Cory's Shearwaters Calonectris diomedea on Selvagem Grande. Ringing & Migration, 20(2), 107-110.
[4] Soave, G. E., Coria, N., Silva, P., Montalti, D., & Favero, M. (2000). Diet of cape petrel Daption capense chicks on South Shetland Islands, Antarctica. Acta ornithologica, 35(2), 191-196.
[5] ACAP. 2009. ACAP Species Assessment: Tristan Albatross Diomedea dabbenena. Available at: #http://www.acap.aq/acap-species/download-document/1206-tristan-albatross#.
[6] Menkhorst, P. W., Pescott, T. W., & Gaynor, G. F. (1984). Results of banding White-faced storm-petrels, Pelagodroma marina at Mud Islands, Victoria. Corella, 8(3), 53-60.
[7] Ollason, J. C., & Dunnet, G. M. (1978). Age, experience and other factors affecting the breeding success of the Fulmar, Fulmarus glacialis, in Orkney. The Journal of Animal Ecology, 961-976.
[8] Garnett, S., Szabo, J., & Dutson, G. (2011). The action plan for Australian birds 2010. CSIRO publishing.
[9] Chastel, O., Weimerskirch, H., & Jouventin, P. (1995). Influence of body condition on reproductive decision and reproductive success in the blue petrel. The Auk, 112(4), 964-972.
[10] Scott, D.A. (1970) The breeding biology of the Storm Petrel *Hydrobates pelagicus*. Unpubl. D.Phil. Thesis, Oxford University
[11] Marchant, S., Higgins, P. (1990). Handbook of Australian, New Zealand and Antarctic Birds: Ratites to Ducks. Melbourne, Oxford University Press.
[12] Bried, J., & Bolton, M. (2005). An initial estimate of age at first return and breeding in Madeiran Stormpetrels Oceanodroma castro. Atlantic Seabirds, 7(2), 71-74.
[13] U.S. Fish and Wildlife Service. 2018. Species status assessment report for the Black-capped petrel (Pterodroma hasitata). Version 1.0. April, 2018. Atlanta, GA.
[14] SCHREIBER EA & J BURGER (eds) (2002) Biology of marine birds. CRC Press, Boca Raton, Florida, USA. 722pp.
[15] David Fletcher, Henrik Moller, Rosemary Clucas, Corey Bragg, Darren Scott, Paul Scofield, Christine M. Hunter, Ilka Win, Jamie Newman, Sam McKechnie, Justine De Cruz, Philip Lyver, Age at First Return to the Breeding Colony and Juvenile Survival of Sooty Shearwaters, The Condor: Ornithological Applications, Volume 115, Issue 3, 1 August 2013, Pages 465–476,
[16] Heather BD, Robertson HA 1996. The Field Guide to the Birds of New Zealand. Viking, Auckland
[17] Thomson, R. B., Alderman, R. L., Tuck, G. N., & Hobday, A. J. (2015). Effects of climate change and fisheries bycatch on shy albatross (Thalassarche cauta) in southern Australia. PLoS One, 10(6), e0127006.
[18] Terauds, A., Gales, R., Baker, G. B., & Alderman, R. (2006). Population and survival trends of Wandering Albatrosses (Diomedea exulans) breeding on Macquarie Island. Emu-Austral Ornithology, 106(3), 211-218.
Booth, Andrea M. (1996). THE BREEDING ECOLOGY OF THE NORTH ISLAND LITTLE SHEARWATER, Puffinus assimilis haurakiensis.
[19] MS thesis in Ecology. Retrieved from the Massey University Database.

Table S4. AFB data included in the PGLS models and sources.

| | Scheme one (Loci-by-loci – Only PartitionFinder2) | Scheme two (SWSC-EN+ PartitionFinder2) |
|---|---|---|
| Matrix used | 95 % | 75 % |
| Number of partitions | 1696 | 12313 |
| Best-fitting substitution model (no of partitions) | GTR - 711 | GTR - 5062 |
| | GTR+G – 92 | GTR+G - 5403 |
| | GTR+I+G - 893 | GTR+G+I - 1848 |

Table S5. Partitioning schemes (one and two) results.

| | Left | Core | Right |
|---|---|---|---|
| GTR | 1608 | 1876 | 1686 |
| GTR+G | 2136 | 1547 | 1838 |
| GTR+I+G | 509 | 738 | 662 |

Table S6. Best-fitting model for each partition within scheme two.

| | Marginal likelihood (strict clock) | Marginal likelihood (relaxed) |
|---|---|---|
| HKY | 833108 | 1165179 |
| HKY+G | 1111895 | 765270 |
| HKY+G+I | 73193 | 38134 |
| GTR | -47424 | -47439 |
| GTR+G | -46895 | -46890 |
| GTR+G+I | -46846 | -46941 |

Table S7. Clock performance under different substitution models.

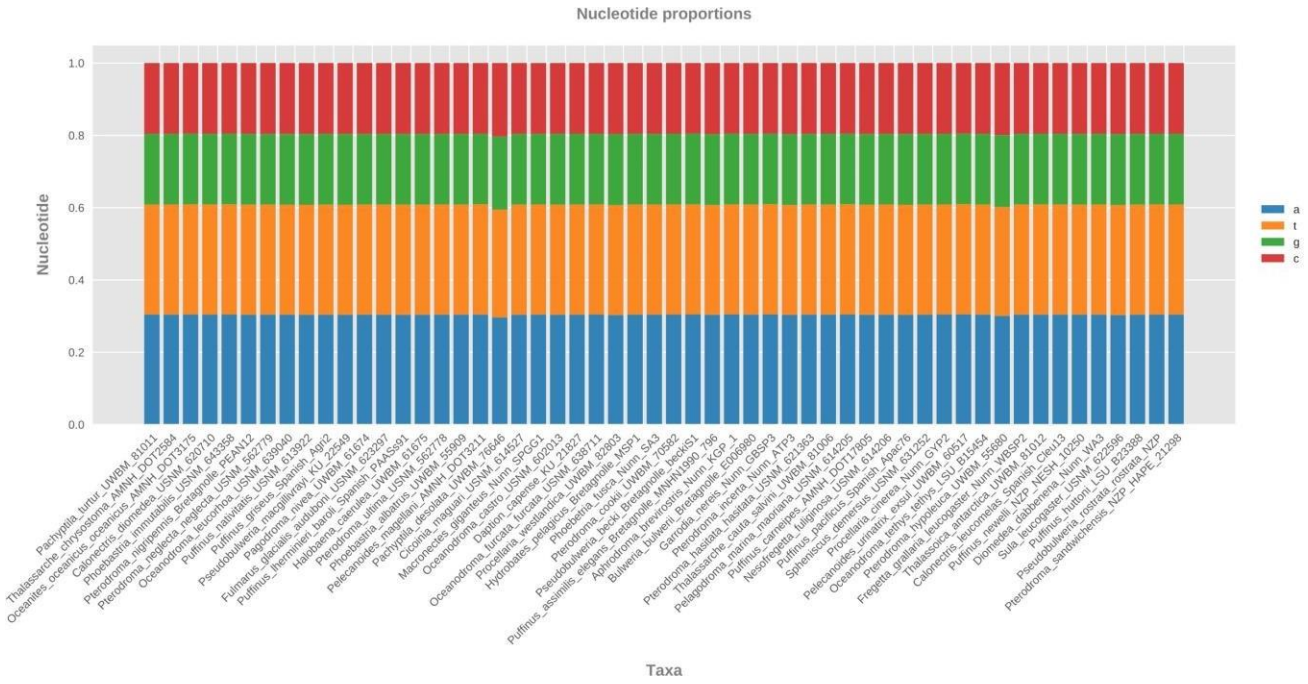


Figure S1. Nucleotide content per species. Created with the Trifusion package.

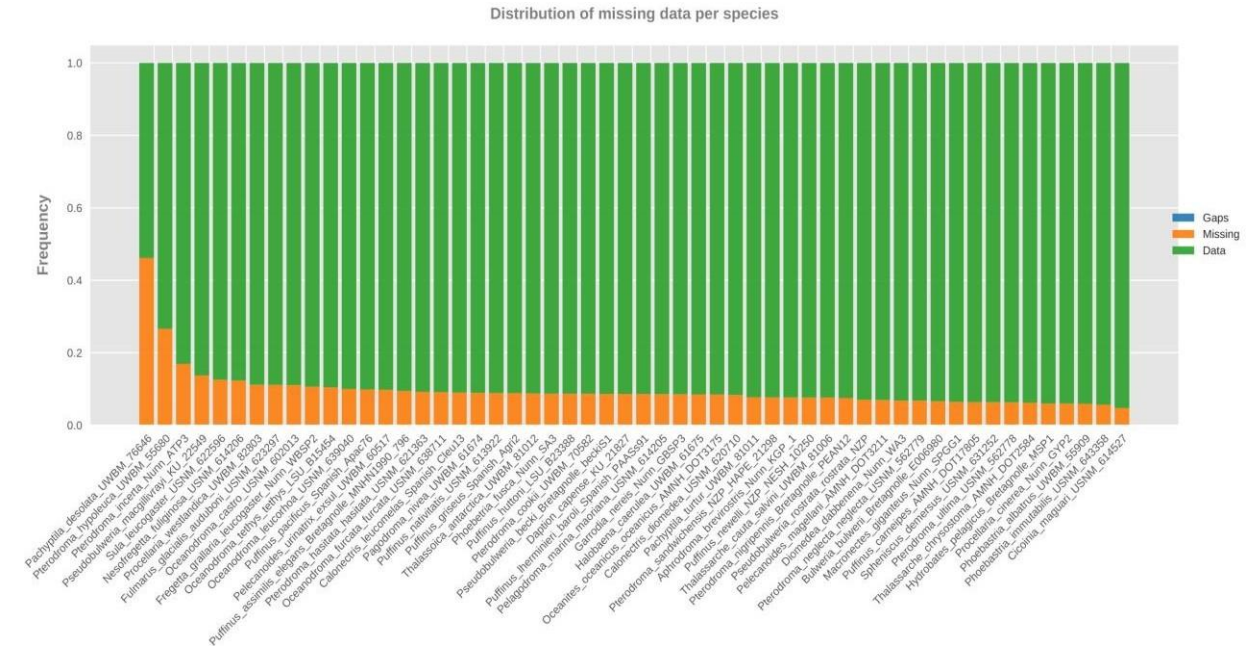


Figure S2. Distribution of missing data per species. *Pachyptila desolata* shows the greatest frequency (approximately 30% of missing data). The percentage of missing data is relative to the complete assembly of concatenated UCEs. Created with the Trifusion package.

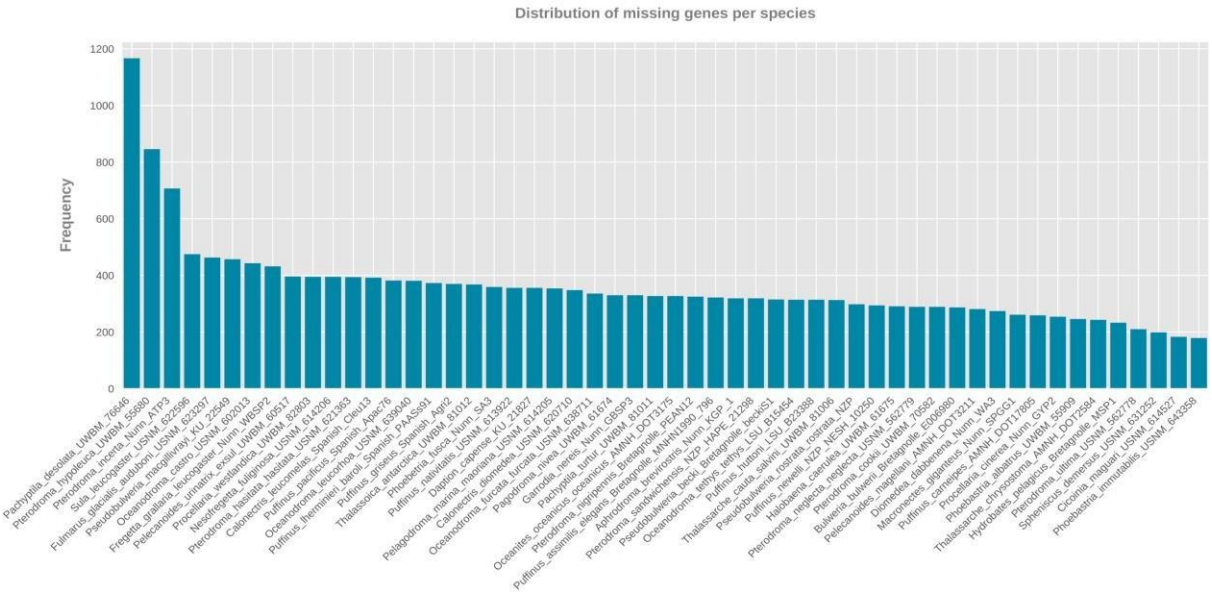


Figure S3. Distribution of missing loci per sample. Out of 4356 loci,*Pachyptila desolata* lacks 1180 loci. Created with the Trifusion package.

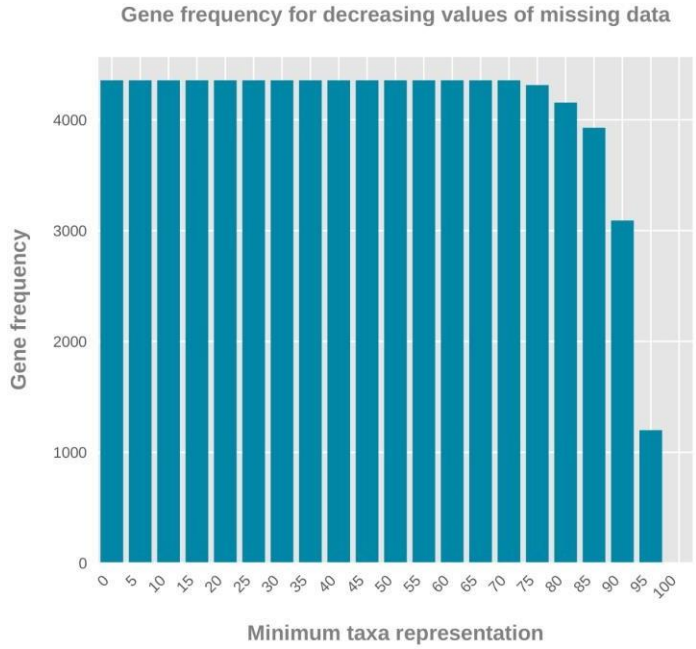


Figure S4. Minimum taxa representation against loci frequency. Created with the Trifusion package.

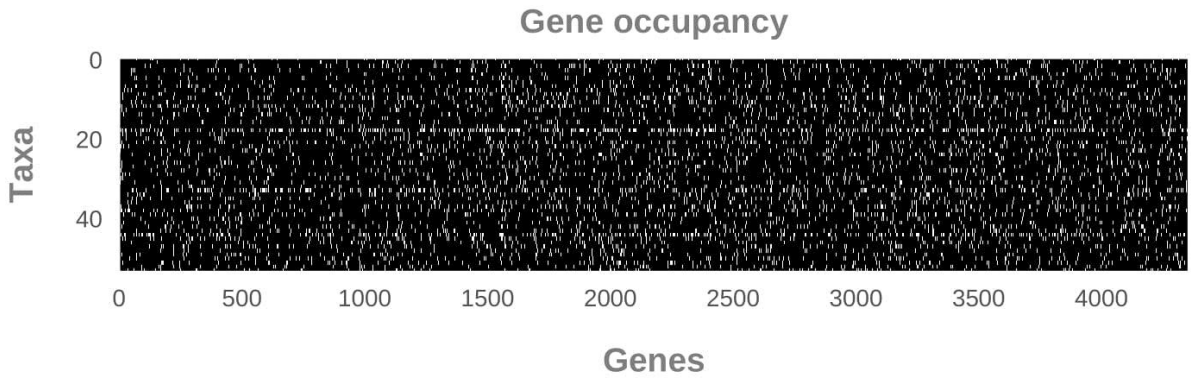


Figure S5. Loci position in the alignment (75% matrix) against taxa. Black shows the presence of loci and white missing loci. Plot created with the Trifusion package.

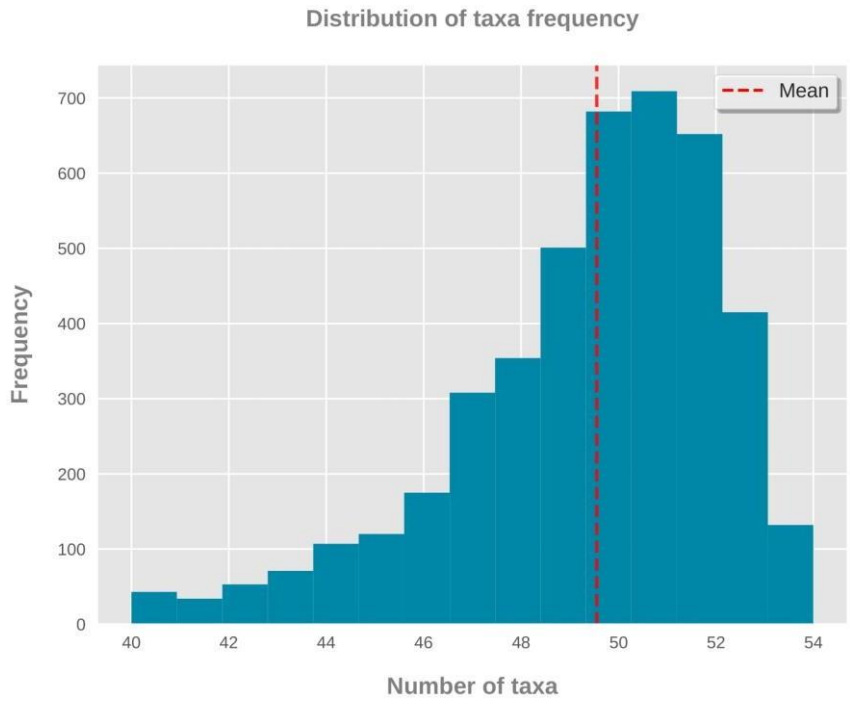


Figure S6. Distribution of taxa frequency. Created with the Trifusion package.

Figure S7. IQ-tree resulting topology.

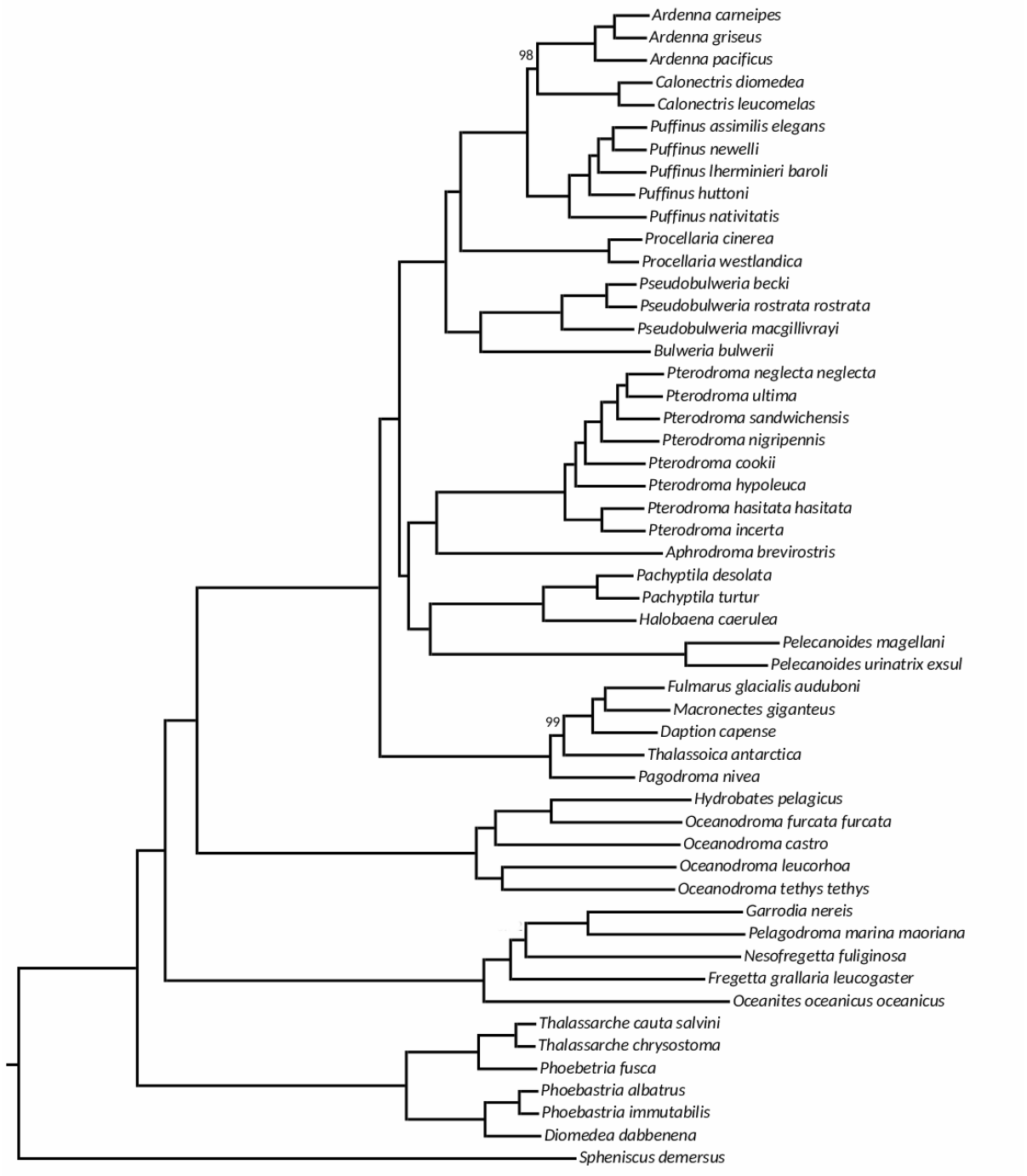

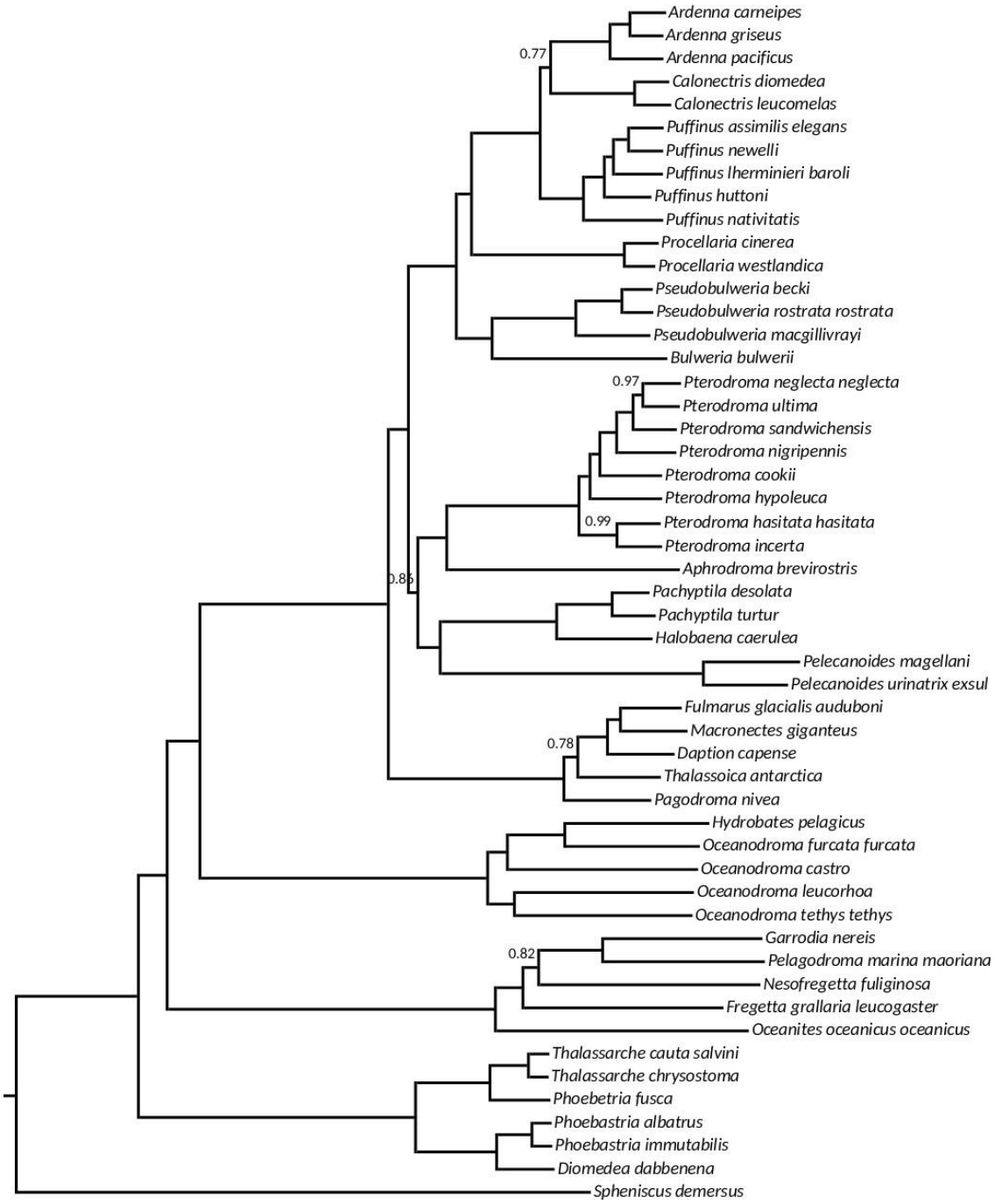


Figure S8. Species tree (ASTRAL-III).

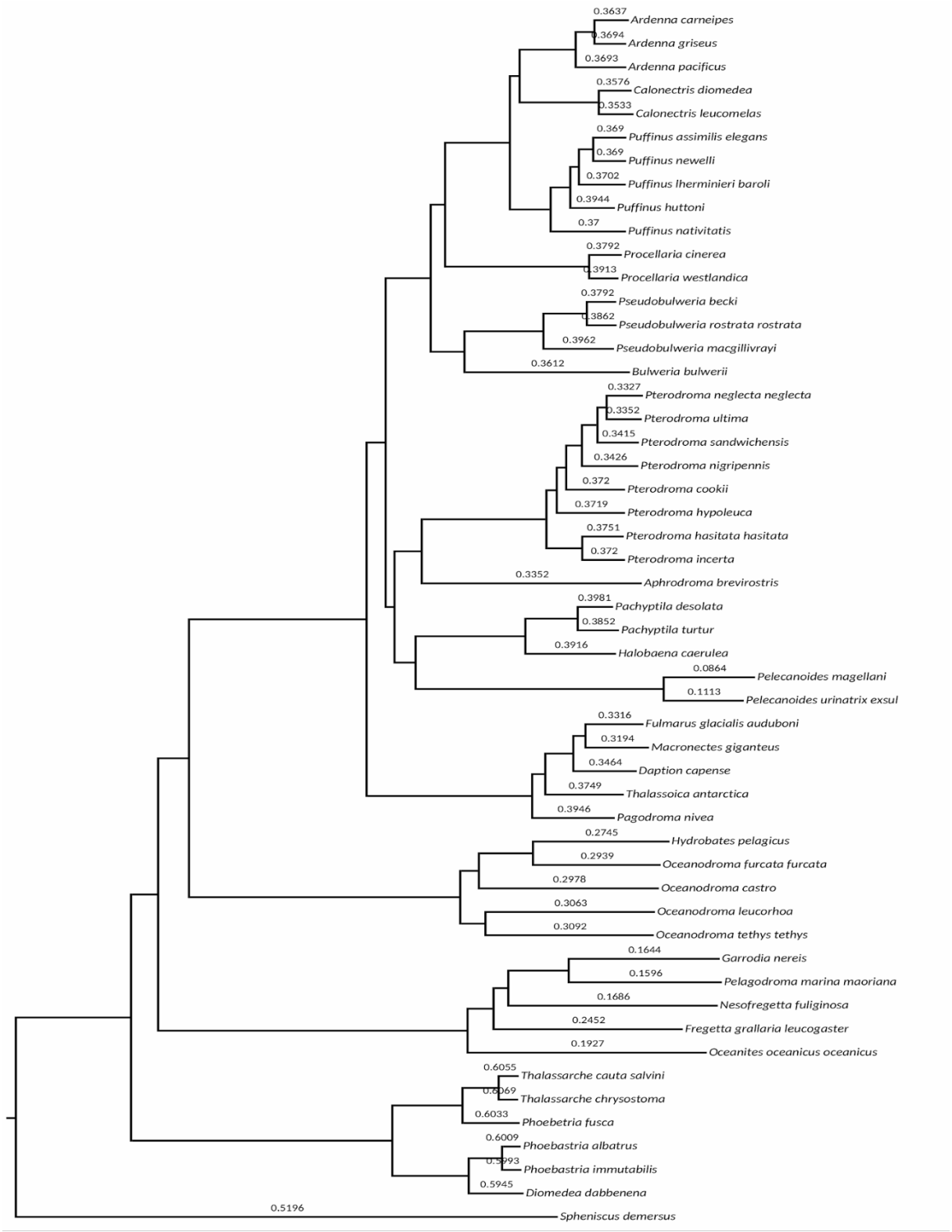


Figure S9. Node heights (Exabayes tree) calculated with Figtree

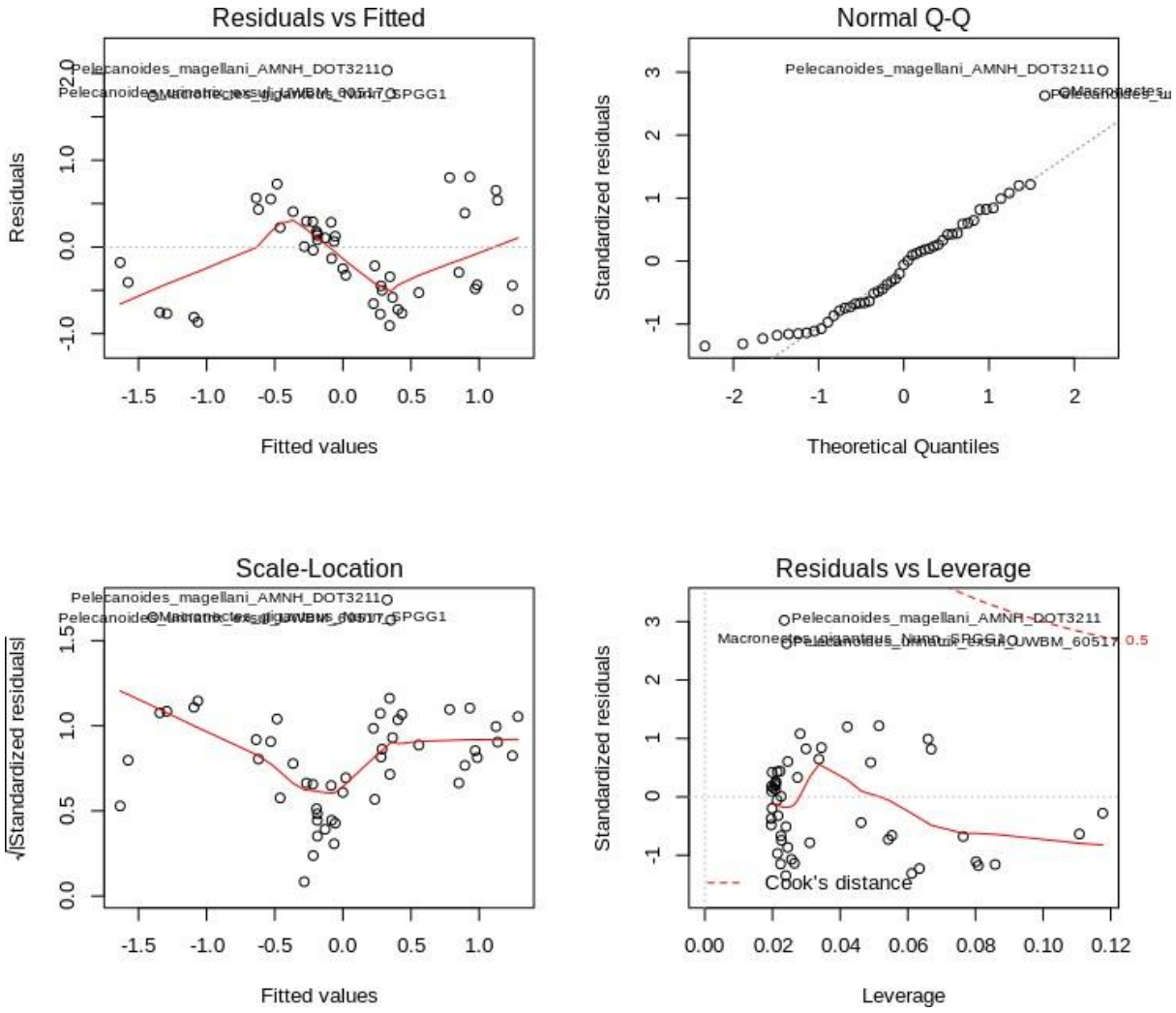


Figure S10. Statistics of the weight dataset.

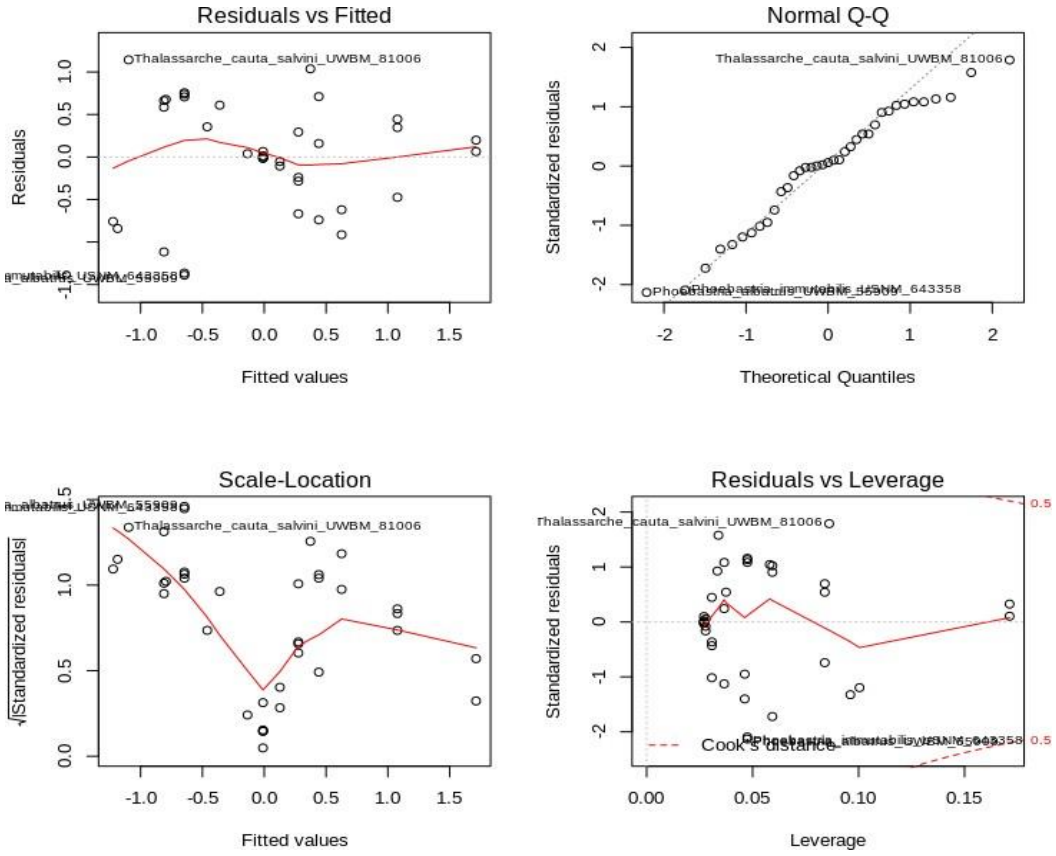


Figure S11. Statistics of the age dataset for the age variable

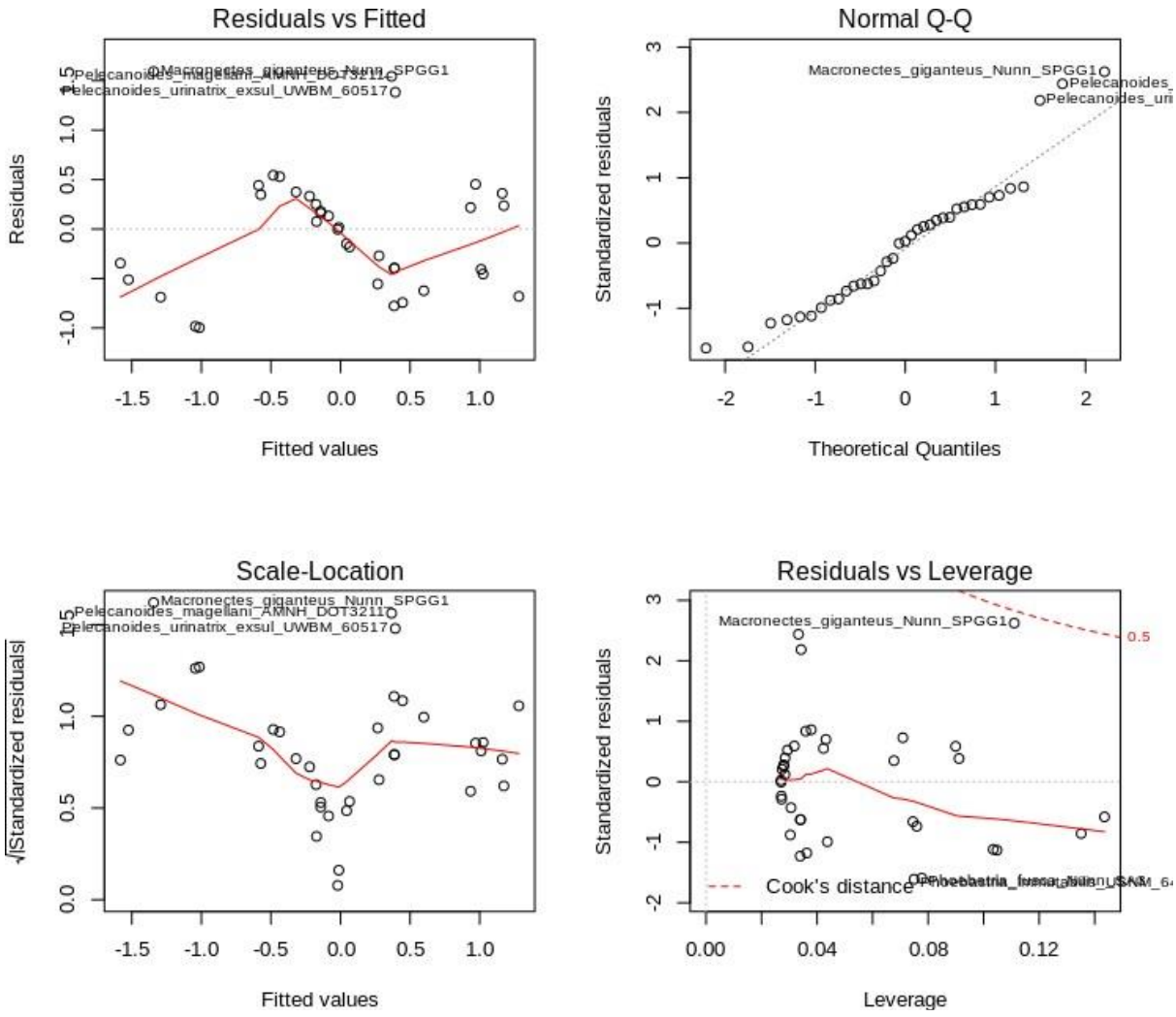


Figure S12. Statistics of the age dataset for the weight variable

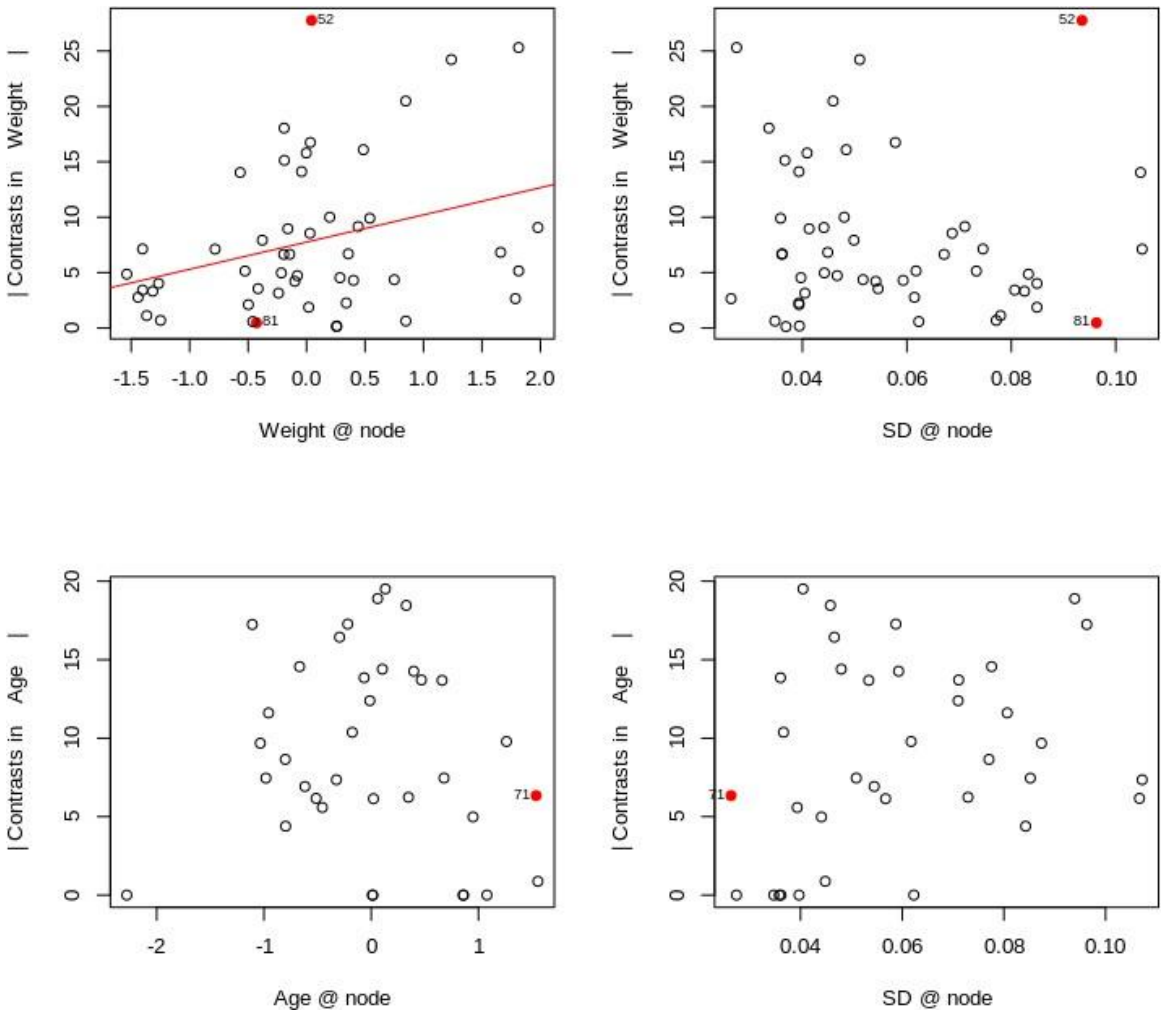


Figure S13. Contrasts and deviation standard in node heights. First row belongs to the weight dataset and second row to age dataset. Red points represent outliers and numbers indicate the node.

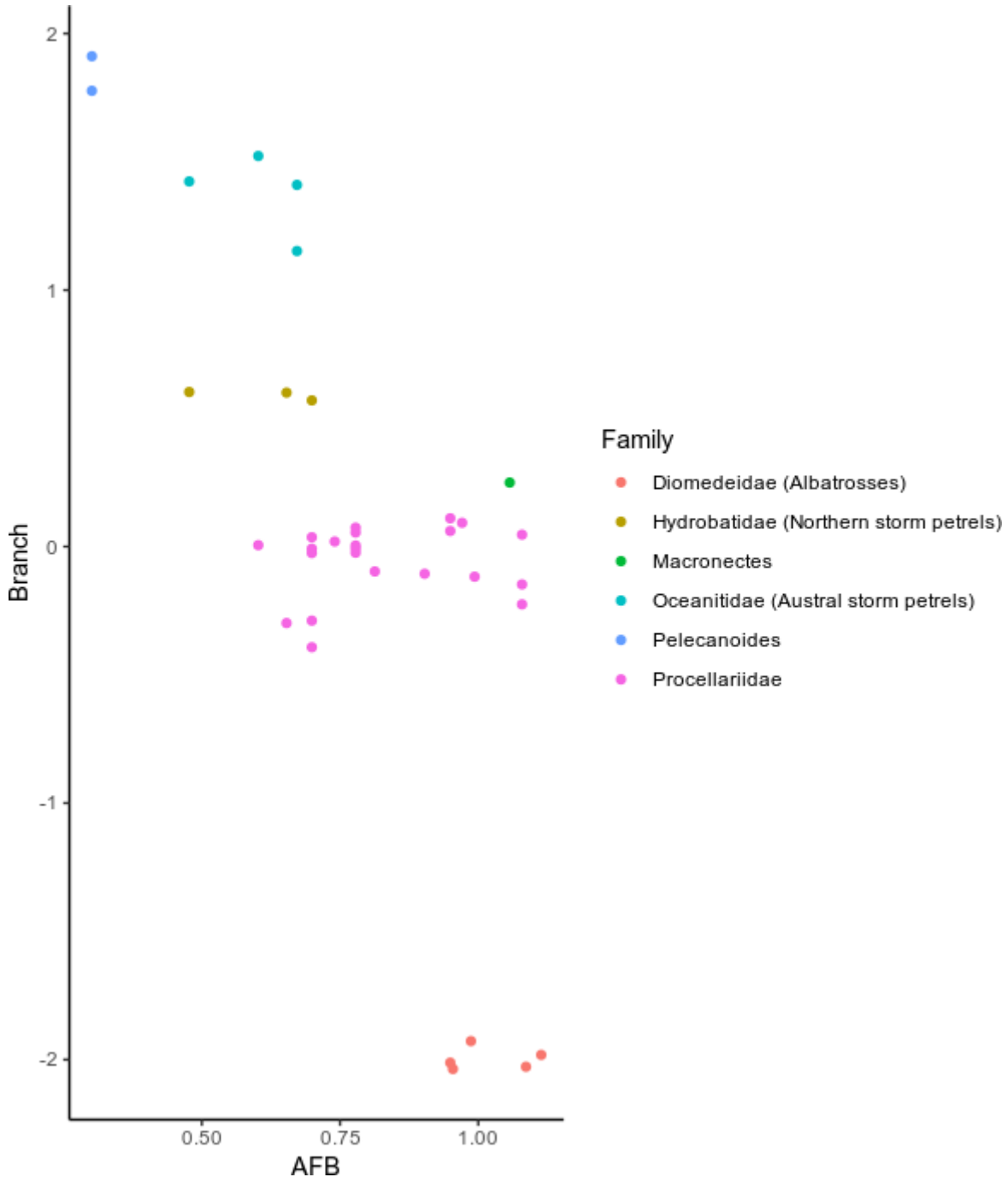


Figure S14. Branch (z-scaled) against AFB by family.

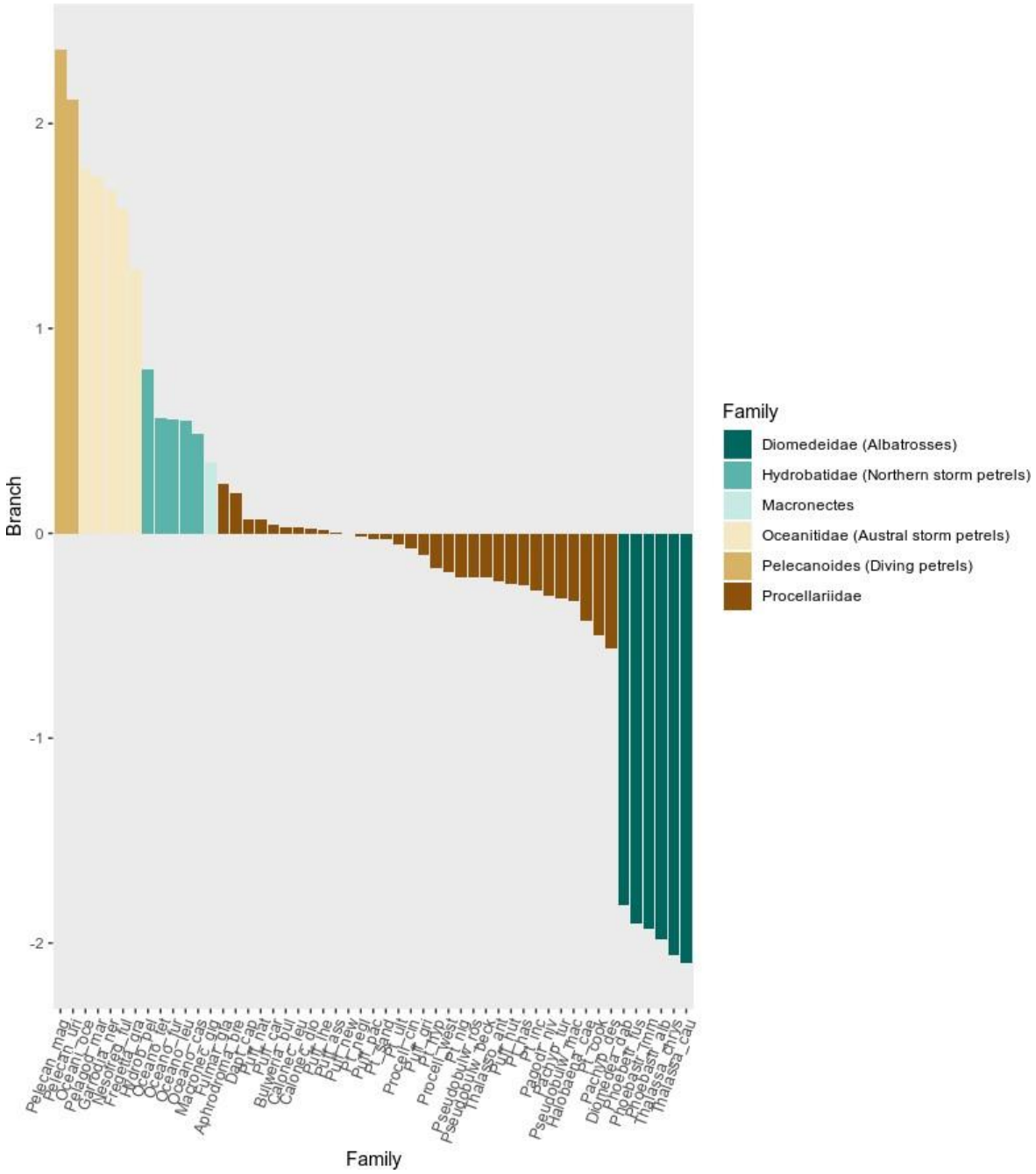


Figure S15. Branch (z-scaled) by family.